# Mechanistic Insights in Transfer Hydrogenation Catalysis by $[Ir(cod)(NHC)_2]^+$ Complexes with Functionalized *N*-Heterocyclic Carbene ligands.

*M. Victoria Jiménez,* Javier Fernández-Tornos, Jesús J. Pérez-Torrente,* Francisco J. Modrego, Pilar García-Orduña, and Luis A. Oro*

Departamento de Química Inorgánica, Instituto de Síntesis Química y Catálisis Homogénea-ISQCH, Universidad de Zaragoza-C.S.I.C., 50009-Zaragoza, Spain.

AUTHOR EMAIL ADDRESS vjimenez@unizar.es, perez@unizar.es

RECEIVED DATE

**Abstract**

The synthesis of unbridged biscarbene iridium(I) $[Ir(cod)(MeIm\cap Z)_2]^+$ complexes having N- or O-functionalized NHC ligands (∩Z = 2-methoxybenzyl, pyridin-2-ylmethyl and quinolin-8-ylmethyl) is described. The molecular structures of the complexes show an antiparallel disposition of the carbene ligands that minimize the steric repulsions between the bulky substituents. However, the complexes were found to be dynamic in solution due to the restricted rotation about the C(carbene)-Ir bond that results in two interconverting diasteromers having different disposition of the functionalized NHC ligands. A rotational barrier of around 80 kJ $mol^{-1}$ (298 K) has been determined by 2D EXSY NMR spectroscopy. The iridium(III) dihydride complex $[IrH_2(MeIm\cap Z)_2]^+$ (∩Z = pyridin-2-ylmethyl) has been prepared by reaction of the corresponding iridium(I) complex with molecular hydrogen. These complexes efficiently catalyzed the transfer hydrogenation of cyclohexanone using 2-propanol as hydrogen source and KOH as base at 80 °C with average TOFs of 117-155 $h^{-1}$ at 0.1 mol% iridium catalyst loading. All the catalyst precursors showed comparable activity independent both of the wingtip type at the NHC ligands or the counterion. Mechanistic studies support the involvement of diene free bis-NHC iridium(I) intermediates in these catalytic systems. DFT calculations have shown that a MPV-like concerted mechanism (Meerwein-Ponndorf-Verley mechanism), involving the direct hydrogen transfer at the coordination sphere of the iridium center, might compete with the well-established hydrido mechanism. Indirect evidence of a MPV-like mechanism has been found for the catalyst precursor having NHC ligands having with a pyridin-2-ylmethyl wingtip.

## Introduction

Heteroditopic ligands of hemilabile character have attracted much attention in recent years due to their potential for catalyst design by tuning the coordination sphere of the metal center. It is well known that functionalized ligands, such as phosphine and N-heterocyclic carbenes (NHCs), with labile bonding groups can play a dual role in a catalyst since they can easily enable coordinative sites at the metal center and, at the same time, protect the coordination sites by a dynamic "on and off" chelating effect.[1] In particular, functionalized NHC ligands have the advantageous property of combining the strong electron-donor ability of the carbene moiety, which form a strong bond to metal centers, with the lability of the donor function that allows for the stabilization of transient intermediates in organometallic catalysts.[2,3] In this context, a large number of complexes containing functionalized NHC ligands have been synthesized and the hemilabile character of several NHC ligands having O, N or S- donor functions has been demonstrated.[4] Interestingly, the active role of the hemilabile fragment has been identified in several catalytic processes.[5]

NHC ligands have been increasingly used in the design of hydrogen transfer catalysts.[6] It has been found that, in contrast to phosphine-based catalysts, iridium-NHC complexes are more active than their Rh-NHC analogues and accordingly, a number of highly efficient neutral and cationic NHC iridium catalysts have been recently reported.[7] In particular, air-stable Ir(III) NHC-based complexes were found to be active catalysts for transfer hydrogenation of ketones, aldehydes, and imines at low catalyst loading.[8] It has been evidenced that the catalyst efficiency in transfer hydrogenation of ketones by sterically demanding unsymmetrically *N,N'*-substituted benzimidazol-2-ylidene [IrBr(cod)(NHC)] complexes was improved when using NHC ligands having a 2-

methoxyethyl substituent.[9] In the same way, highly effective iridium(I) hydrogen transfer catalysts based on unsymmetrical 2-methoxyphenyl donor-functionalized expanded ring NHCs have been recently reported.[10] Thus, it becomes evident that the presence of a hemilabile fragment on the catalyst structure has a considerable impact on hydrogen transfer catalytic activity.

Late transition metal catalyzed transfer hydrogenation of unsaturated substrates has been explained through different mechanisms involving both monohydride or dihydride species, according to an inner-sphere mechanism, or concerning the participation of a ligand in the catalytic reaction, according to an outer sphere metal-ligand bifunctional catalysis mechanism.[11] However, in the case of Ir(I) complexes, the monohydride mechanism seems to be preferred.[12] Mechanistic studies on cationic complexes having a methoxy-functionalized NHC ligand (NHC∩Z, type I, Chart 1), in combination with DFT calculations, allowed us to disclose that the interaction of the MeO- fragment of the NHC ligand with an alcoxo intermediates species facilitates the β-H elimination step in route to the key hydrido [IrH(cod)(NHC∩Z)] intermediate species.[13] On the other hand, bridged bis-NHC ligands have proven to be very useful for the tuning of the electronic and steric properties of the metal centers. [M(bis-NHC)(OAc)$I_2$][8f] (type II, Chart 1) and $[M(cod)(bis\text{-}NHC)]^{+}$,[14] (type III, Chart 1) complexes, having M(III) and M(I) metal centers (M = Rh, Ir), respectively, have also been shown to be efficient catalysts for transfer hydrogenation although no mechanistic investigations have been performed so far. In contrast, the catalytic activity of unbridged biscarbene $[M(cod)(NHC)_2]^{+}$ complexes in hydrogen transfer reactions remains unexplored.

The aim of this work is to synthesize iridium(I) $[Ir(cod)(NHC\cap Z)_2]^{+}$ complexes having two N- or O-functionalized NHC ligands (type IV, Chart 1) in order to evaluate

their catalytic activity in transfer hydrogenation of ketones. The presence of two uncoordinated donor functions in these catalyst precursors should facilitate the stabilization of coordinatively unsaturated catalytic intermediates. In addition, from a mechanistic point of view, a direct hydrogen transfer mechanism where the hydrogen transfer takes place between an alkoxide ligand and a ketone simultaneously coordinated to the iridium center, Meerwein-Ponndorf-Verley mechanism (MPV), could be operative in these systems due to the presence of two strongly bonded NHC ligands. In fact, computational studies have given support to the MPV mechanism for some iridium catalysts.[15]

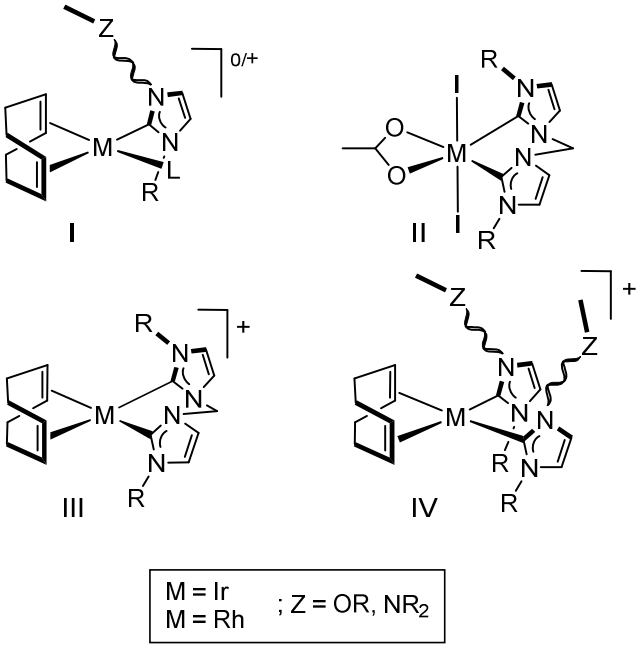


**Chart 1.** Mono- and bis-NHC metal complexes as hydrogen transfer catalysts (M = Rh, Ir).

## Results and Discussion

**Synthesis of Precursors for Hemilabile NHC Ligands.** The imidazolium salts precursors for selected O- and N-donor rigid functionalized N-heterocyclic carbene ligands (Chart 2) were prepared by alkylation of 1-methylimidazole with the corresponding functionalized alkyl bromide. The salt 1-(2-methoxybenzyl)-3-methyl-1*H*-imidazol-3-ium bromide (**1**)[13] was synthesized by alkylation of 1-methylimidazole with 2-methoxybenzyl bromide, prepared by bromination of 2-methoxybenzyl alcohol,[16] in toluene following the procedure described for the *N*-*tert*-butyl derivative.[17] In the same way, 1-(pyridin-2-ylmethyl)-3-methyl-1*H*-imidazol-3-ium bromide (**2**) was prepared using 2-(bromomethyl)pyridine as alkylating reagent.[18] 1-(Quinolin-8-ylmethyl)-3-methyl-1*H*-imidazol-3-ium hexafluorophosphate (**3**) was prepared following the procedure described by Webster and Li.[19]

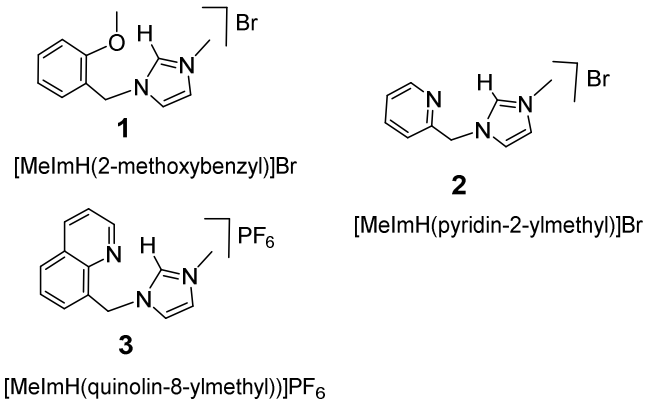


**Chart 2.** Imidazolium salts precursors for functionalized NHC ligands.

Unbridged bis-carbene $[M(cod)(NHC)_2]^+$ complexes are accessible by several specific synthetic methods, as for example, the double NHC transfer under halide abstraction using $[Ag(NHC)_2]NTf_2$[20] or imidazolium-2-carboxylate adducts ($NHC\text{-}CO_2$)[21] as transmetalation agents. However, the use of alkoxo ligands or external alkoxide bases as

deprotonating agents of the imidazolium salts,[22,23,24] has proved to be especially useful for the preparation of the target iridium(I) $[Ir(cod)(NHC\cap Z)_2]^+$ complexes. In contrast, the use of silver $[(NHC\cap Z)AgX]_n$[25] complexes as transmetalation agents resulted in the formation of complex mixtures that contain the neutral $[IrX(cod)(NHC\cap Z)]$ compounds.

Complexes [Ir(cod){MeIm(2-methoxybenzyl)}$_2$]Br (**4·Br**) and [Ir(cod){MeIm(pyridin-2-ylmethyl)}$_2$]Br (**5·Br**) have been synthesized applying the Herrmann's method slightly modified,[22] *via* deprotonation of the imidazolium salts **1** and **2** by the bridging ethoxo ligands in the dimer $[Ir(\mu\text{-}OEt)(cod)]_2$, generated in situ by reaction of $[Ir(\mu\text{-}Cl)(cod)]_2$ with NaH in ethanol, in the presence of an excess of NaOEt (Scheme 1). The complexes were obtained as yellow-orange microcrystalline solids in good yield after extraction with dichloromethane and crystallization with n-hexane. The corresponding hexafluorophosphate salts, **4·PF$_6$** and **5·PF$_6$**, were prepared by metathesis of the bromide salts with $NaPF_6$ in dichloromethane. The application of the Herrmann's methodology to the bromide salt of the quinolin-8-ylmethyl imidazolium derivative resulted in the formation of **6·Br** in low yield. However, the *in situ* deprotonation of the hexafluophosphate imidazolium salt **3** by the strong base KO$^t$Bu, and further reaction with $[Ir(\mu\text{-}Cl)(cod)]_2$ directly afforded [Ir(cod){MeIm(quinolin-8-ylmethyl)}$_2$]$PF_6$ (**6·PF$_6$**), which was isolated as an orange microcrystalline solid in 80% yield.

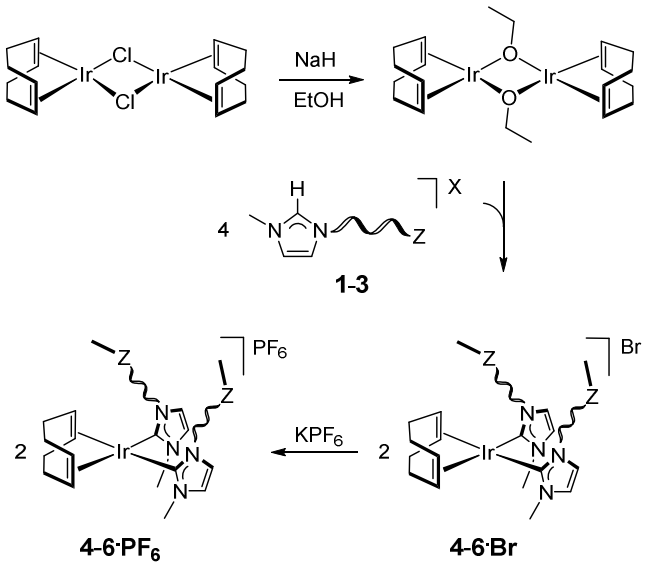


**Scheme 1.** General method for the preparation of $[Ir(cod)(NHC\cap Z)_2]^+$ (NHC∩Z = functionalized NHC ligand) complexes **4**–**6**$^+$.

The iridium(I) $[Ir(cod)(NHC\cap Z)_2]X$ (∩Z = 2-methoxybenzyl, **4**; pyridin-2-ylmethyl, **5**; quinolin-8-ylmethyl, **6**; X = Br or $PF_6$) complexes have been fully characterized by elemental analysis, mass spectrometry and multinuclear NMR spectroscopy. The MALDI-Tof mass spectra showed the molecular ions with the correct isotopic distribution and in some cases those derived of the loss of the cod and/or NHC∩Z ligands. Conductivity measurements of solutions of the complexes in acetone agreed with the presence of 1:1 electrolytes. In addition, the IR spectra of complexes **4-6·PF$_6$** showed a broad strong band corresponding to the stretching vibrations of the $PF_6^-$ anion (840 $cm^{-1}$), and the characteristic septet resonance for the $PF_6^-$ anion was observed in the $^{31}P\{^1H\}$ NMR spectra at around $\delta$ -144 ppm.

The $^1H$ NMR of the complexes exhibited duplicated resonances for both cod and NHC ligands, which evidenced the presence of two isomers. As an example, the $^1H$ NMR (acetone-$d^6$) of **4**$^+$ displays two AB quartets for the diastereotopic >$CH_2$ protons

of the 2-methoxybenzyl wingtips at δ 5.54 and 5.39 ($J_{H-H}$ = 15 Hz) ppm which suggest that the NHC∩Z ligands are equivalent in both isomers. Furthermore, the presence of two resonances for the =CH protons of the cod ligand for both species also supports the existence of two symmetrical isomers. This situation is also reflected in the $^{13}C\{^1H\}$ NMR that displays two low field resonances at δ 178.41 and 178.28 ppm for the carbene carbon atoms of both isomers. The spectroscopic data are in agreement with the existence of two diasteromers for these complexes derived from the relative disposition of the functionalized NHC ligands: the *up-down* isomer ($C_2$ symmetry) and the *up-up* isomer ($C_s$ symmetry) having antiparallel and parallel arrangement of the carbene ligands, respectively (Figure 1).

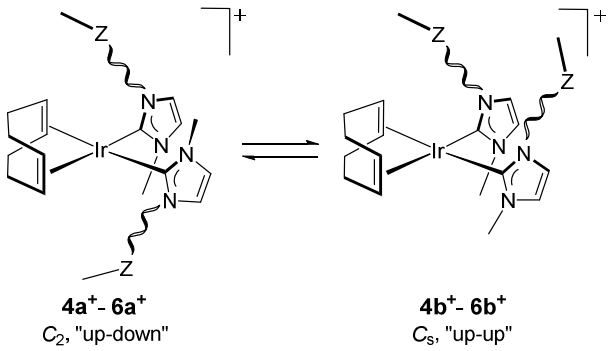


**Figure 1**. Equilibrium between the two diasteromers of complexes $[Ir(cod)(MeIm\cap Z)_2]^+$ (**4**$^+$–**6**$^+$).

Reliable assignment for the $^1H$ and $^{13}C\{^1H\}$ resonances of both diasteromers was achieved by combination of the $^1H$-$^1H$ COSY, $^{13}C$ APT and $^1H$-$^{13}C$ HSQC spectra. Interestingly, the bidimensional $^1H$-$^1H$-NOESY spectra of the complexes show strong exchange cross-peaks between all types of protons for both species, together with weak NOE cross-peaks, indicating that both diasteromers interconvert in solution (Figure 1).

As can be seen in the selected region of the $^{1}$H-$^{1}$H NOESY NMR spectrum of **5**·**Br** in $CD_2Cl_2$ at 300 K (Figure 2) exchange cross-peaks between the >$CH_2$ and -Me resonances of the 1-(pyridin-2-ylmethyl)-3-methyl-imidazol-2-carbene ligands and the =CH resonances of the cod ligands for both isomers are apparent. The bidimensional spectrum also allows for the univocally identification of the diasteromers. Thus, the major isomer shows proximity NOE cross-peaks between the proton H6 of the pyridine wingtip and the methyl protons of the NHC∩Z ligands, which is in agreement with the antiparallel arrangement of both ligands in the *up-down* isomer **5a**$^{+}$. As expected, this cross-peak is not observed for the minor isomer **5b**$^{+}$ having parallel NHC∩Z ligands. (Figure 2 and Supporting Information).

The diasteromer ratio **4a**$^{+}$/**4b**$^{+}$ in $CD_2Cl_2$ is close to that found in acetone-$d^6$, 1.38 and 1.22, respectively, at the same temperature (298 K). However, the ratio for **5**$^{+}$ is strongly influenced by the solvent. The *up-down* diastereomer is more abundant in $CD_2Cl_2$, **5a**$^{+}$/**5b**$^{+}$ ratio of 2.3, than in acetone-$d^6$, where a ratio of 1.2 was measured. Finally, **6a**$^{+}$/**6b**$^{+}$ ratios of 1.86 and 1.42 were found in $CDCl_3$ and $CD_2Cl_2$, respectively.

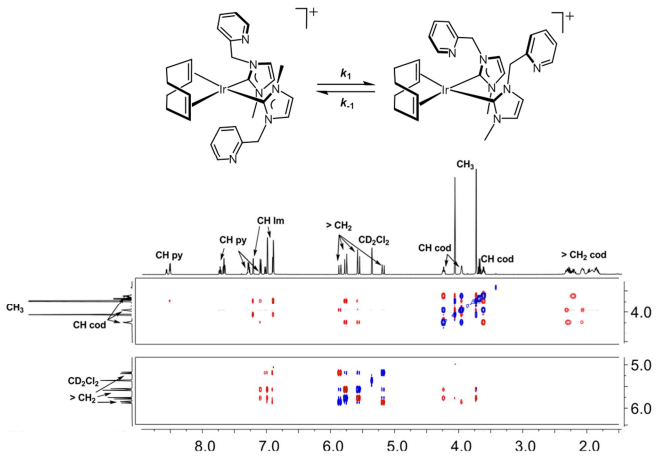


**Figure 2.** Sections of 2D $^{1}$H-$^{1}$H-NOESY ($CD_2Cl_2$, 300 K) NMR spectrum for complex **5**·**Br**.

**Kinetic studies**. The interconversion between the *up-down* and *up-up* diasteromers of complexes $\mathbf{4}^{+}$-$\mathbf{6}^{+}$ requires the rotation of the NHC∩Z ligands about the Ir-C bond. Experimental rotational rates for **5·Br** were obtained from magnetization transfer experiments using 2D EXSY NMR spectroscopy. This method has been increasingly applied to the study of dynamic processes, determination of rotational barriers and conformational analysis.[26] The basis of a quantitative 2D EXSY experiment is the relationship between the intensity of the exchange cross-peaks and the rate constants for chemical exchange. The forward and backward exchange rate constants, $k_1$ and $k_{-1}$, for the equilibrium $\mathbf{5a}^{+} \leftrightarrows \mathbf{5b}^{+}$ were determined by integration of the cross-peaks between the methyl resonances of the 1-(pyridin-2-ylmethyl)-3-methyl-imidazol-2-ylidene ligands in both interconverting species in the $^{1}$H 2D-EXSY NMR spectra. The kinetic parameters for the equilibrium $\mathbf{5a}^{+} \leftrightarrows \mathbf{5b}^{+}$ at four different temperatures are summarized in Table 1.

The temperature influence on the exchange reaction rate was investigated in the temperature range 300-330 K in $CD_2Cl_2$ and the activation parameters determined by linear least-squares fit using the logarithmic form of the Eyring equation. The kinetic parameters obtained from the Eyring plot were $\Delta H_1^{\#} = 74.8 \pm 4.1$ kJmol$^{-1}$ and $\Delta S_1^{\#} = -11 \pm 13$ JK$^{-1}$mol$^{-1}$, and $\Delta H_{-1}^{\#} = 77.0 \pm 4.2$ kJmol$^{-1}$ and $\Delta S_{-1}^{\#} = -11 \pm 13$ JK$^{-1}$mol$^{-1}$ (see Supporting Information). Noteworthy, the small negative value of the entropy term is in agreement with an intramolecular interconversion process. The activation barriers for the forward ($\Delta G_1^{\#}$) and reverse ($\Delta G_{-1}^{\#}$) processes were $\Delta G_1^{\#} = 78 \pm 8$ kJmol$^{-1}$ and $\Delta G_{-1}^{\#} = 80 \pm 8$ kJmol$^{-1}$, respectively (298.15 K).

On the other hand, the calculated equilibrium constants, *K*, obtained from the determined rate constants ($K_{EXSY} = k_1/k_{-1}$) are in good agreement with the experimental values, $K_{INT}$, obtained from the same sample by integration of both methyl resonances in an experiment recorded with the same relaxation time. The estimated equilibrium constant $K_{INT}$ ranges only between 2.36–2.10 in the temperature range under study. Interestingly, the ln*K* vs 1/T plot gave a linear fit leading to the following thermodynamic parameters: $\Delta H^o$ = -3.4 kJmol$^{-1}$ and $\Delta S^o$ = -4.0 Jmol$^{-1}$ (See Supporting Information).

The rotational barriers of *ca.* 80 kJmol$^{-1}$ found in complex **5**$^+$ are higher than those found in some [RhX(diene)(NHC)] complexes which are in the range 65–70 kJmol$^{-1}$.[27,28] Evidence for the steric origin of the bond rotation barrier has been recognized,[29] and in fact, hindered C(carbene)-Rh rotation at room temperature has been observed both in complexes [RhX(diene)(NHC)] and [Rh(cod)(NHC)$_2$]$^+$ having NHC ligands with bulky substituents.[23,30] The dynamic behavior exhibited by our complexes is certainly unexpected due to the presence of two bulky functionalized NHC∩Z ligands that should hinder the rotation about the Ir-C bond. Likely the rotational process involves the concerted motion of both NHC ligands with assistance of the cod ligand or the NHC wingtip through a highly distorted transition state.

**Table 1.** 1H 2D EXSY-derived rate constants (k1 and k-1/s-1) and calculated equilibrium constants (K) for the equilibrium **5a**$^+$ ⇆ **5b**$^+$.[a]

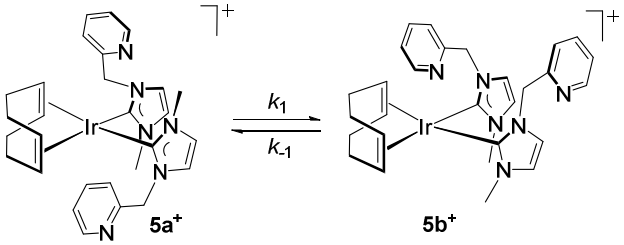

| T (K) | $k_1$ ($s^{-1}$)[b] | $k_{-1}$ ($s^{-1}$)[b] | $K_{EXSY}$ [c] | $K_{INT}$ [c] |
|---|---|---|---|---|
| 300 | 0.16 | 0.07 | 2.29 | 2.36 |
| 310 | 0.45 | 0.21 | 2.14 | 2.29 |
| 320 | 1.19 | 0.57 | 2.11 | 2.19 |
| 330 | 2.66 | 1.26 | 2.10 | 2.10 |

[a] 2D-EXSY NMR spectra (500 MHz) were recorded using a concentrate solution of **5**$^+$ in $CD_2Cl_2$ with an optimized mixing time of 500 ms. [b] The integrals for the exchange cross-peak were processed using the EXSYCalc program to obtain the rate constants $k_1$ and $k_{-1}$. c $K_{EXSY}$, calculated equilibrium constants from EXSY determined rate constants ($k_1/k_{-1}$); $K_{INT}$, experimental equilibrium constants obtained from the integration of the methyl resonances in the $^1$H NMR spectra.

**Structural studies**. The structure of the cationic complexes **4**$^+$–**6**$^+$ was also confirmed by X-ray analysis on single crystals obtained by slow diffusion of diethyl ether into a concentrated solution of the complexes in acetone. The molecular structures of the **4**·**PF$_6$**, **5**·**Br** and **6**·**PF$_6$** salts have been determined, and a view of the corresponding cations is depicted in Figure 3. The most representative bond lengths and angles are collected in Table 2.

The asymmetric unit of **5**$^+$ includes two crystallographically independent but chemically identical molecules. Both of them, together with those of complexes **4**$^+$ and **6**$^+$, share several common structural features, in particular, the antiparallel disposition of both NHC∩Z ligands, i.e. the *up-down* diasteromer. In all of them, the metal atom is coordinated to the carbon atoms of two NHC∩Z ligands and to the two olefinic bonds of a cyclooctadiene molecule, in a slightly distorted square-planar environment. Coordination angles formed by the carbenic carbon atoms and the centroid of the diolefines are close to 90°. Deviations from this magnitude are found in the bite angle of cod ligands, whose values are close to the mean value found in Ir(cod) fragments in mononuclear square-planar complexes (85.9(10)º).[31] The presence of the olefin places

the NHC ligands in a relative *cis* position, contrary to the preferred *trans* disposition observed in iridium complexes with two symmetrical monodentate NHC ligands where $C_{carbene}$-Ir-$C_{carbene}$ angles bigger than 160º are found.[32] The C(9)-Ir-C(12) angles are also slightly different from 90º, with a mean value of 94.19(2)º, and the two carbene heterocycles are nearly perpendicular, as reported in $[Ir(cod)(NHC)_2]$[20] and $[Ir(cod)(MeImPz)_2]$[24] (Pz = pyrazolyl) complexes. These features, together with the *up-down* disposition of the carbene ligands, minimize the steric repulsions between the bulkiest substituents on the NHC∩Z carbene ligands, which are located as far away as possible. The Ir-$C_{carbene}$ bond distances, in the range 2.045(3)-2.078(12) Å, were found to be similar to those of Ir(I)-$(NHC)_2$ complexes as well as related iridium(I)-NHC complexes containing substituents in the carbene ligand with possible hemilabile characteristics.[20,23a,24,33]

Dihedral angles between the planes of the NHC∩Z carbene ligands and the metal coordination mean plane measured in these structures are of 80.5(4)º and 78.1(4)º for complex $\mathbf{4}^+$; 71.9(2), 77.2(2), 77.4(2) and 75.9(2)º for $\mathbf{5}^+$; and 81.47(9) and 82.57(10)º for $\mathbf{6}^+$. These values agree with those observed in $[RhCl(ICy)_2(PPh_3)]$ (ICy = 1,3-dicyclohexylimidazol-2-ylidene) (78.6 and 79.2º)[34] and $[Ir(cod)(ICy)_2]$ (78.0 and 75.3º)[22a] complexes, where the NHC carbene ligands are relatively *trans*- and *cis*-located, respectively. Considering Ir and Rh complexes having bidentate methylene-bridged bis-NHC ligands it is noteworthy that the dihedral angles γ found in complexes $\mathbf{4}^+$, $\mathbf{5}^+$ and $\mathbf{6}^+$ are larger than those reported in complexes with one $>CH_2$ bridge [8f,25,35,36] but similar to those with longer chains ($(CH_2)_n$; n = 3 or 4). [22a,37]

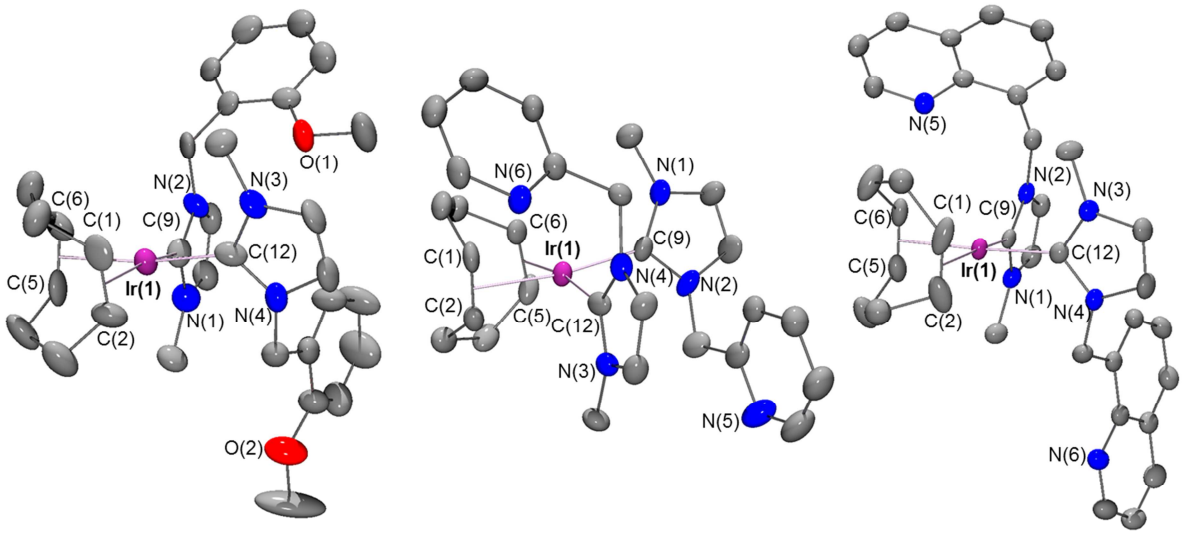


**4**$^{+}$ **5**$^{+}$ **6** $^{+}$

**Figure 3.** View of the cations of complexes **4**·$\mathbf{PF_6}$, **5**·**Br** and **6**·$\mathbf{PF_6}$. Hydrogen atoms have been omitted for clarity.

**Table 2.** Selected bond lengths (Å) and angles (º).

| | **4**$^{+}$ | **5**$^{+}$ | | **6**$^{+}$ |
|---|---|---|---|---|
| Ir(1)-M(1)[a] | 2.097(10) | 2.086(8) | 2.088(7) | 2.076(3) |
| Ir(1)-M(2)[a] | 2.067(16) | 2.096(7) | 2.079(8) | 2.074(3) |
| Ir(1)-C(9) | 2.078(12) | 2.058(7) | 2.045(7) | 2.045(3) |
| Ir(1)-C(12) | 2.061(13) | 2.062(7) | 2.047(6) | 2.045(3) |
| M(1)-Ir(1)-M(2) | 86.0(6) | 85.2(3) | 86.1(3) | 85.94(12) |
| M(1)-Ir(1)-C(9) | 171.9(5) | 171.9(3) | 171.3(3) | 174.70(11) |
| M(1)-Ir(1)-C(12) | 89.8(5) | 90.7(3) | 91.4(3) | 90.68(12) |
| M(2)-Ir(1)-C(9) | 90.6(5) | 90.7(3) | 89.3(3) | 90.23(10) |
| M(2)-Ir(1)-C(12) | 170.4(6) | 170.6(3) | 169.6(3) | 174.93(10) |
| C(9)-Ir(1)-C(12) | 94.6(5) | 94.4(3) | 94.4(3) | 93.39(9) |
| N(1)-C(9)-N(2) | 106.1(10) | 103.8(6) | 103.5(6) | 104.1(2) |
| N(3)-C(12)-N(4) | 104.9(11) | 104.1(6) | 103.8(5) | 104.1(2) |

[a] M(1) and M(2) are the midpoints of olefinic C(1)=C(2) and C(5)=C(6) bonds, respectively.

**Synthesis of [IrH$_2${κ$^2$*C,N*-MeIm(pyridin-2-ylmethyl)}$_2$]PF$_6$ (7·PF$_6$)**. The cationic bis-NHC∩Z iridium(I) complexes **4**–**6**$^+$ did not react with molecular hydrogen at room temperature. However, under more forcing conditions of pressure and temperature reaction was observed in all cases although only complex **5**$^+$ gave a clean reaction product. Probably the higher coordination ability of the pyridine fragment compared to quinoline or methoxy might be responsible of the difference in the reactivity. Reaction of **5**·**PF$_6$** with dihydrogen at 10 bar and 60 °C for 48 hours gave a pale yellow solution from which the iridium(III) dihydride complex [IrH$_2${κ$^2$*C,N*-MeIm(pyridin-2-ylmethyl)}$_2$]PF$_6$ (**7**·**PF$_6$**) was isolated as a pale yellow solid in 81 % yield. Complex **7**$^+$ results from the oxidative addition of hydrogen, hydrogenation of the 1,5-cyclooctadiene ligand and release of cyclooctene, which was detected by GC/MS analysis of the reaction mixture (Scheme 2).

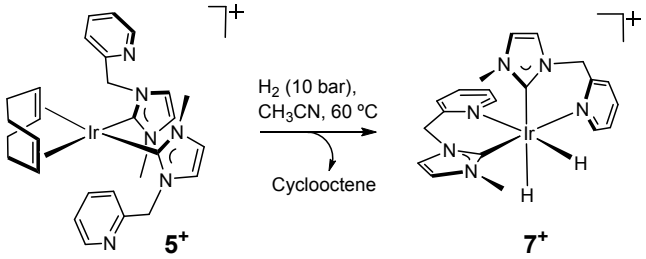


**Scheme 2**. Synthesis of [IrH$_2${κ$^2$*C,N*-MeIm(pyridin-2-ylmethyl)}$_2$]$^+$ (**7**$^+$).

Complex **7**$^+$ is conductor in acetone and the MS mass spectra displays the molecular ion at *m/z* of 541.2. The $^1$H NMR spectrum of **7**$^+$ in CD$_3$CN showed the absence of the typical resonances of the cod ligand and the presence of two high field doublet resonances at δ –9.60 and –20.12 ppm for the two hydrido ligands. The magnitude of the $J_{H\text{-}H}$ coupling constant of 5.6 Hz is indicative of a mutually *cis* disposition of both

hydrido ligands. In addition, the spectra show no equivalent NHC ligands, which is consistent with an unsymmetrical structure with the hydrido ligands having very different *trans* ligands. Thus, compound $\mathbf{7}^+$ is an unsymmetrical iridium(III) octahedral complex having two 1-(pyridin-2-ylmethyl)-3-methyl-imidazol-2-ylidene ligands $\kappa^2$-*C*,*N* coordinated (Scheme 2). The sterochemistry of $\mathbf{7}^+$ has been univocally established with the help of the two-dimensional $^1$H-$^1$H-NOESY spectrum of a $CD_3CN$ solution of $\mathbf{7}^+$ due to the presence of proximity cross peaks of the hydrido resonances with protons of different fragments of the molecule (Figure 4).

The hydrido ligand at $\delta$ –9.60 ppm presents NOE effect with the H6 proton of pyridine fragment of a NHC ligand and with the bridging methylene of the other, which suggest that is located *trans* to the carbenic atom carbon of the first one. In contrast, the hydrido ligand at $\delta$ –20.12 ppm should be the one located *trans* to pyridine as it presents NOE effect with the methyl substituent of the same NHC ligand and with the bridging methylene resonance of the second (Figure 4). The large upfield shift of the hydrido resonance *trans* to pyridine ligand compared to the one *trans* to the carbene is in agreement with that found for related dihydrido octahedral iridium complexes having an abnormal NHC ligand derived from 2-pyridylmethylimidazolium salts.[38]

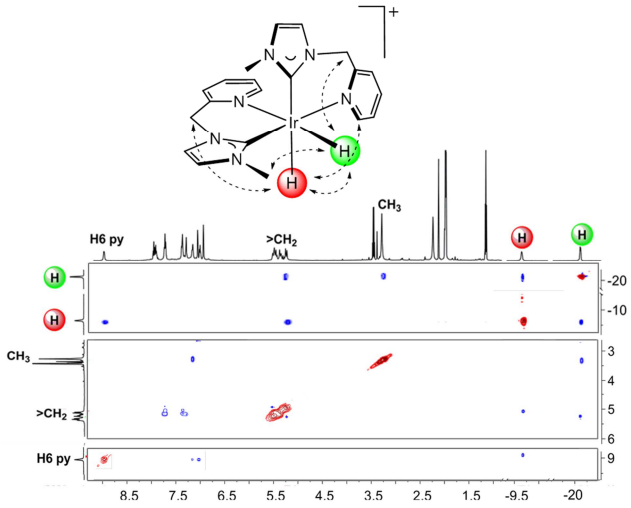


**Figure 4**. $^{1}$H-$^{1}$H-NOESY ($CD_3CN$, 300 K) NMR spectrum of $[IrH_2\{\kappa^2C,N$-MeIm(pyridin-2-ylmethyl)$\}_2]^+$ (**7**$^+$).

**Hydrogen Transfer Catalysis by [Ir(cod)(MeIm∩Z)$_2$]X (X = Br, PF$_6$) Complexes**. The cationic complexes having two N- or O-functionalized NHC ligands, $[Ir(cod)(MeIm\cap Z)_2]^+$ (**4**$^+$-**6**$^+$), have been tested as catalysts for transfer hydrogenation of cyclohexanone using 2-propanol as hydrogen source and KOH as base. The influence of the wingtip fragment of the NHC ligand, 2-methoxybenzyl (**4**$^+$), pyridin-2-ylmethyl (**5**$^+$) or quinolin-8-ylmethyl (**6**$^+$), and the counter anion (X = Br$^-$ or $PF_6^-$), in the catalytic activity has been investigated. The obtained results under optimized standard conditions for related catalytic systems,[13] catalyst/cyclohexanone/base ratio of 1/1000/5 at 80 °C, are summarized in Table 3.

**Table 3.** Hydrogen Transfer from 2-Propanol to Cyclohexanone Catalyzed by $[Ir(cod)(MeIm\cap Z)_2]X$ (X = Br, $PF_6$).[a,b]

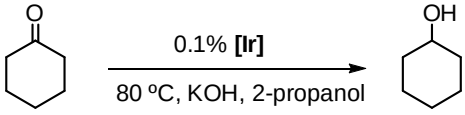

| entry | catalyst | time (min) | conversion (%) | TON | TOF[c]/h$^{-1}$ | $TOF_{50}$[d]/h$^{-1}$ |
|---|---|---|---|---|---|---|
| 1 | **4**·Br | 480 | 94 | 941 | 118 | 578 |
| 2 | **4**·$PF_6$ | 475 | 92 | 922 | 117 | 588 |
| 3 | **5**·Br | 395 | 93 | 932 | 142 | 887 |
| 4 | **5**·$PF_6$ | 380 | 94 | 943 | 149 | 909 |
| 5 | **6**·$PF_6$ | 420 | 91 | 910 | 130 | 652 |
| 7 | **7**·$PF_6$ | 370 | 95 | 954 | 155 | 462 |

[a] Reaction conditions: catalyst/cyclohexanone/base: 1/1000/5, $[Ir]_0 = 1 \times 10^{-3}$ M in 2-propanol at 80 °C. [b] The reactions were monitored by GC using mesitylene as internal standard. [c] Average turnover frequency (mol of product/mol of catalyst per hour) determined at the reaction time. [d] $TOF_{50}$ calculated at 50% conversion of cyclohexanone.

The cationic $[Ir(cod)(MeIm\cap Z)_2]^+$ complexes showed a moderate catalytic activity in the reduction of cyclohexanone. The required time to reach conversions over 95% is 6-8 h with average TOFs of 117-155 h$^{-1}$. As can be seen in Table 3, the counterion ($Br^-$ or $PF_6^-$) has little influence on the catalytic activity (entries 1-2 and 3-4) thereby evidencing that the coordinating ability of the bromide anion does not hinder the catalytic activity. It is noticeable that the three catalysts show comparable activity independent of the wingtip type at the NHC ligands which contrast with that observed for iridium(I) complexes having only one NHC∩Z ligand. In fact, we have shown that complexes having O-functionalized NHC ligands provide much more active systems than the corresponding N-functionalized ligands.[13] In this series, complex **5**$^+$ having NHC ligands with a pyridin-2-ylmethyl wingtip is slightly more active than the rest with an average TOF and $TOF_{50}$ values of 149 and 909 h$^{-1}$, respectively.

The reaction profiles for the hydrogen transfer reduction of cyclohexanone catalyzed by the cationic complexes **4**$^+$-**6**$^+$ (hexafluorophosphate salts) are shown in Figure 5. Although complex **5**$^+$ exhibits a higher activity up to 70% conversions, the kinetic

profiles are quite similar showing the absence of an induction period for catalyst preactivation which is in accordance with the immediate color change observed when the catalytic mixture is heated at 80 °C.

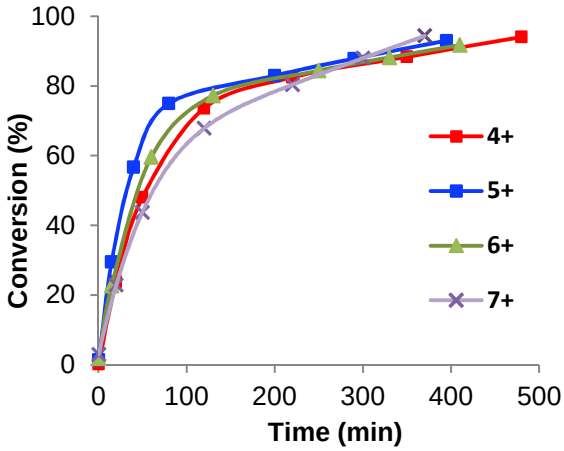


**Figure 5.** Reaction profiles for the catalytic transfer hydrogenation of cyclohexanone using 0.1 % of iridium catalyst (hexafluorophosphate salts) in 2-propanol at 80 ºC and KOH as base.

In general, iridium(I) complexes having only one functionalized NHC ligand exhibited a superior catalytic performance than related bis-NHC complexes. For example, the neutral [IrBr(cod){MeIm(2-methoxibenzyl)}] and cationic $[Ir(NCCH_3)(cod)\{MeIm(2\text{-methoxibenzyl})\}]^+$ complexes, with average TOFs of 824 and 4622 $h^{-1}$, respectively, are considerably more active than $\mathbf{4}^+$ (Table 3, entries 1 and 2). However, $\mathbf{5}^+$ is more active that [IrBr(cod){MeIm(pyridin-2-ylmethyl)}] (31 $h^{-1}$) and shows comparable activity to $[Ir(cod)\{MeIm(pyridin\text{-}2\text{-}ylmethyl)\}]^+$ (248 $h^{-1}$, Table 3, entries 3 and 4).[13]

The dihydride complex $[IrH_2\{\kappa^2C,N\text{-}MeIm(pyridin\text{-}2\text{-}ylmethyl)\}_2]PF_6$ (**7·PF$_6$**) has been prepared in order to assess the possible participation of iridium(III) intermediates

in the hydrogen transfer reduction of cyclohexanone catalyzed by $[Ir(cod)(MeIm\cap Z)_2]^+$ complexes. Complex $\mathbf{7}\cdot\mathbf{PF_6}$ is also an efficient catalyst precursor giving a similar average TOF than $\mathbf{5}\cdot\mathbf{PF_6}$ (Table 3, entry 7) showing a comparable kinetic profile although with a steady increase of the activity after 2 hours. Thus, it seems reasonable to think that under catalytic conditions the active species generated from $\mathbf{7}^+$ is possibly the same than the one formed from $\mathbf{5}^+$. This hypothesis requires the release of the cyclooctadiene ligand of $\mathbf{5}^+$. In fact, the GC/MS analysis of a catalytic test carried out with a substrate/$\mathbf{5}^+$ ratio of 100 evidenced the presence of cyclooctene. Furthermore, the catalytic activity is completely inhibited in the presence of 1,2-bis(diphenylphosphine)ethane (dppe) in the reaction media due to the release of 1,5-cyclooctadiene (GC/MS evidence) and blocking of the accessible coordination sites.

These observations strongly suggest that the generation of the active species from precatalysts $\mathbf{5}^+$ comes from the reduction of 1,5-cyclooctadiene to cyclooctene, likely through the hydrido species $[IrH(cod)(MeIm\cap Z)_2]$, formed by β-H elimination in the neutral alkoxo intermediate $[Ir(OR)(cod)(MeIm\cap Z)_2]$ (∩Z = pyridin-2-ylmethyl). Thus, insertion of the C=C double bond of the cyclooctadiene ligand into the Ir-H bond followed by protonolysis should give the key species $[Ir(OR)(MeIm\cap Z)_2]$ (**8a**) after cyclooctene replacement by an alkoxo ligand. Alternatively, ketone insertion into an Ir-H bond of the dihydrido complex $\mathbf{7}^+$ followed by reductive elimination of the corresponding alcohol and incorporation of an alkoxo ligand, also account for the formation of species **8a** (Figure 6).

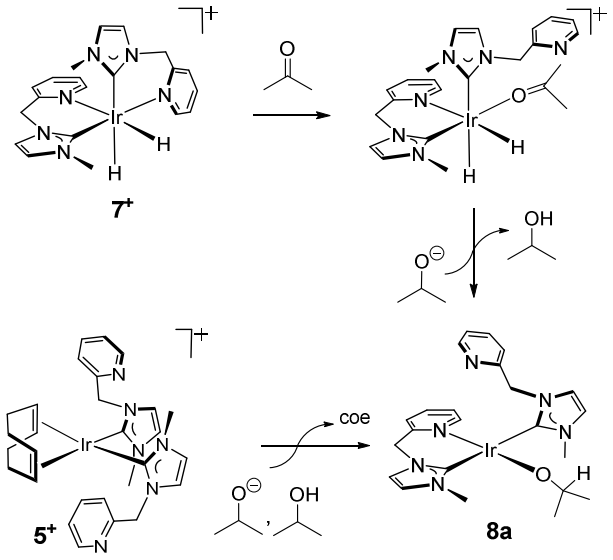


**Figure 6.** Reaction pathways leading to the formation of the catalytic active species [Ir(OR)(MeIm∩Z)$_2$] (**8a**, ∩Z = pyridin-2-ylmethyl from **5**$^+$ or **7**$^+$.

**Mechanism of Transfer Hydrogenation Catalysis by [Ir(cod)(MeIm∩Z)$_2$]$^+$ Complexes Having Functionalized *N*-Heterocyclic Carbene ligands: DFT studies.** In order to explore the possible mechanisms of the hydrogen transfer process by means of DFT calculations two different mechanisms have been considered: the formation of a hydride intermediate via β-elimination and a MPV-like pathway (Meerwein-Ponndorf-Verley mechanism), both starting from the hypothesis of an active catalyst free of cyclooctadiene. Two vacant coordination sites become available after cyclooctadiene elimination as cyclooctene. They could be occupied by an alkoxo or substrate ligands, as well as by the donor atom of the N-substituent on one of the carbene ligands resulting in species similar to **8a** (Figure 6). In order to avoid the conformational freedom of an otherwise uncoordinated sidearm, the catalysts have been somewhat simplified. The ligand ImMe$_2$ (1,3-dimethyl-imidazol-2-ylidene) has been used as a model of one of the two functionalized NHC ligands while the other one has been fully included. In the

following discussion a similar numbering scheme is used for the two investigated NHC∩Z ligands, and when necessary they are distinguished as ***n*a** (*e.g.*: **8a**, ∩Z= pyridin-2-ylmethyl) or ***n*b** (*e.g.*: **8b**, ∩Z = 2-methoxybenzyl), in a particular numbered species.

Starting from precursor **8**, in which the two vacant positions are occupied by an isoproxide ligand and the donor atom of the N-substituent of the carbene ligand, the Figure 7 summarizes the intermediate hydrido complexes devised for a β-elimination pathway. In a first step for this mechanism, β-elimination from the isopropoxide ligand could lead to a pentacoordinated hydrido complex **9**, via **TS 8-9**, with calculated activation energy of 133.5 kJ/mol. The species **9** is not the most stable isomer for this complex, as an isomer with a square planar geometry **13** with the sidearm uncoordinated is 18.7 kJ/mol more stable (Figure 8). In fact, similar pentacoordinate geometry for the complex having a 2-methoxybenzyl substituent has not been found. According to this, a β-elimination pathway with opening of the chelate ring formed by the sidearm of the carbene ligand is envisaged. Scanning back the hydrido reinsertion process starting from the square planar **13** product sheds some light on the possible pathway of the reaction. For this reinsertion process we have found the transition state **TS 12-13**. An IRC analysis shows that this TS connects an agostic intermediate (**12a,** Figure 9, and **12b**) with the hydrido species **13a** and **13b** by very low activation energies of 6.6, and 5.9 kJ/mol, respectively (**a**, ∩Z= pyridin-2-ylmethyl, and **b**, ∩Z = 2-methoxybenzyl, Figure 10). The agostic intermediates **12** show a very elongated C-H and C=O distances, e.g. 1.227 Å and 1.361 Å for **12a**, respectively (Figure 9).[39]

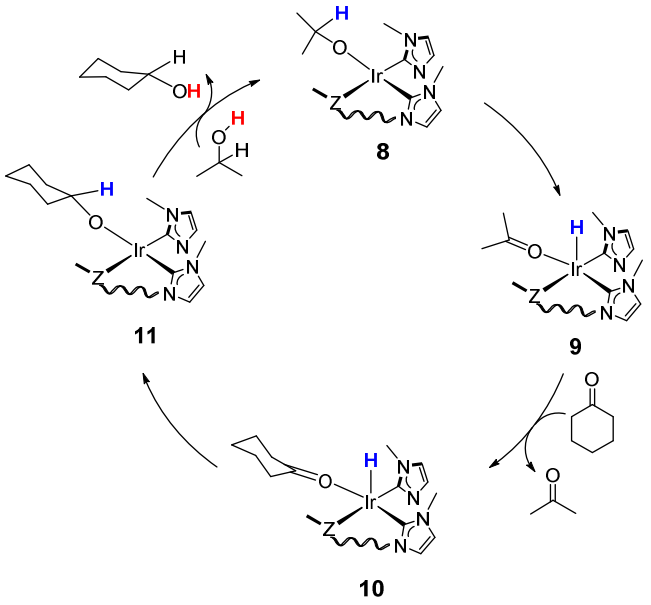


**Figure 7**. Inner sphere mechanism for the transfer hydrogenation by $[Ir(cod)(MeIm\cap Z)_2]^+$ catalysts involving pentacoordinated monohydride intermediates.

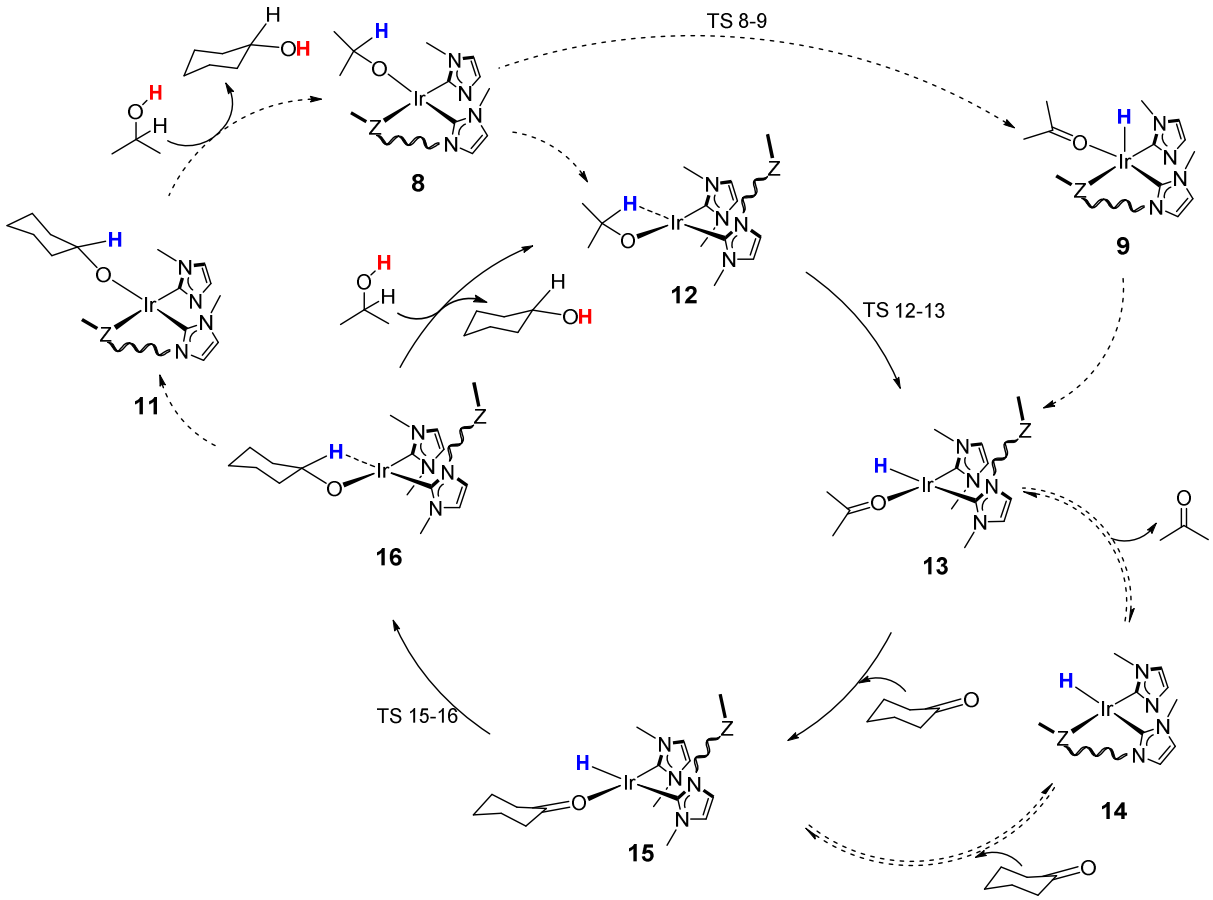

**Figure 8**. Catalytic cycle through hydride square-planar intermediates via β-elimination from isopropoxide. A route allowing for the coordinating ability of the N-substituent on the NHC ligand is depicted (dotted arrows) along with the proposed route (solid arrows). The former is discarded due to the higher energies involved and the differences which should be experimentally observed for different ligands (see text).

Accordingly, this route affords an easier pathway to the hydrido intermediates **13a** and **13b** pointing out that opening of the sidearm should be previous to the β-elimination. This agrees with the mechanistic studies by Hartwig et al.[40] that have found that a dissociative pathway towards β-elimination in square planar iridium alkoxides operates in preference to direct elimination where they propose an structure similar to **12** as a possible transition state.

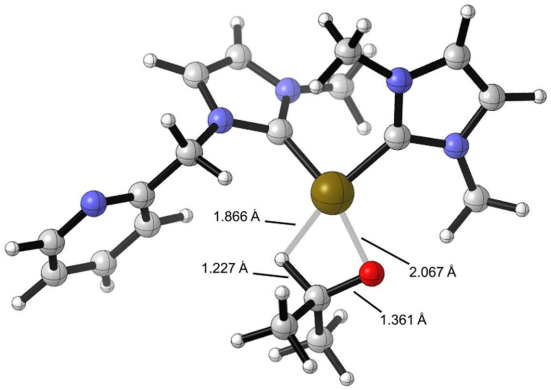


**Figure 9**. Calculated structure for compound **12a** and some representative distances for the isopropoxide-iridium interaction.

The acetone ligand in **13** can be replaced by cyclohexanone or by the sidearm substitutent on the carbene ligand leading to the square planar hydrido complex **14**. Formation of this hydrido complex is slightly exergonic (-4.07 kJ/mol) for the 2-methoxybenzyl complex **14b**, but with a net release of energy of 71.1 kJ/mol for the

pyridin-2-ylmethyl one **14a**, what could represent a resting state in the catalytic cycle. Thus, both species **13** and **14** should be in equilibrium. Given the large excess of cyclohexanone the concentration of **14** should be low in spite of its stability. After replacement of acetone by cyclohexanone (either directly from **13** or through **14**) intermediate **15** is formed. Then, migratory insertion into the Ir–H bond through **TS 15-16** (with energy barriers of 18.1 kJ/mol for **TS 15a-16a**, and 12.8 kJ/mol for **TS 15b-16b**) results in new alkoxo hydride agostic complexes **16a** and **16b**. Substitution of the formed cyclohexanoxide by isopropoxide in an alcoholysis reaction returns the cycle to intermediate **12** rendering cyclohexanol as product, and completing the catalytic cycle through hydride square planar intermediates via β-elimination mechanism (Figures 8 and 10).

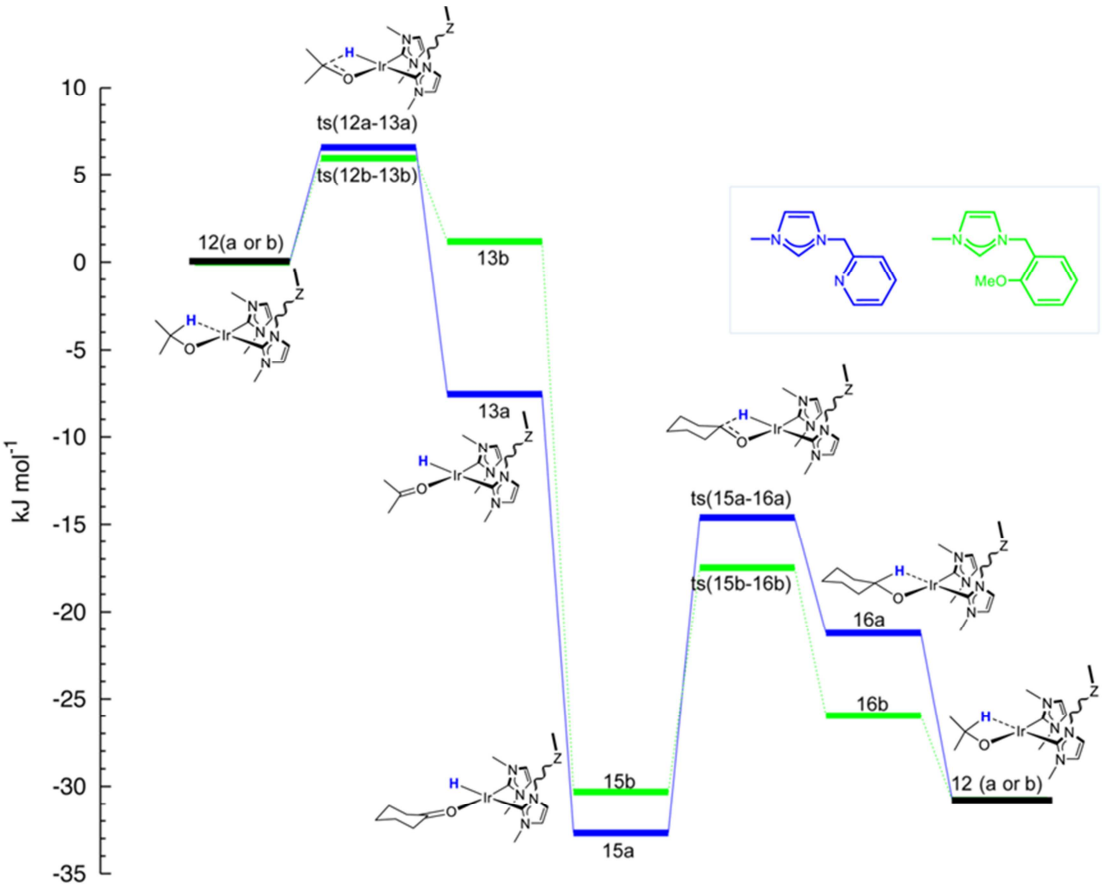

**Figure 10**. Energy profiles for the proposed catalytic cycle involving hydrido species. The "**a**" numbered series refer to the catalyst bearing a pyridin-2-ylmethyl functionalized NHC ligand while the "**b**" series are those referred to the catalyst having a NHC with a 2-methoxybenzyl wingtip.

For a MPV-like mechanism (Figure 11), and also starting from the species **8**, the opening of the chelate ring formed between the carbene donor and the sidearm can lead to the coordination of cyclohexanone rendering the species **17**. In that species, the direct hydrogen atom transfer from the isopropoxide ligand to the cyclohexanone substrate through **TS 17-18** (see Figure 12 for **TS17a-18a**) forms the intermediate **18** from which the cyclohexanol product could be directly produced by alcoholysis. In that calculated transition state, **TS 17-18**, the transferred hydrogen sits between both ligands. Additionally, this step is energetically feasible as the required activation energies are only 31.7 kJ/mol for **TS 17a-18a**, and 52.3 kJ/mol for **TS 17b-18b**. The catalytic cycle can be closed from the acetone-cyclohexanolate species **18** by substitution of cyclohexanoxide by isopropoxide and acetone by cyclohexanone through alcoholysis and addition reactions, respectively.

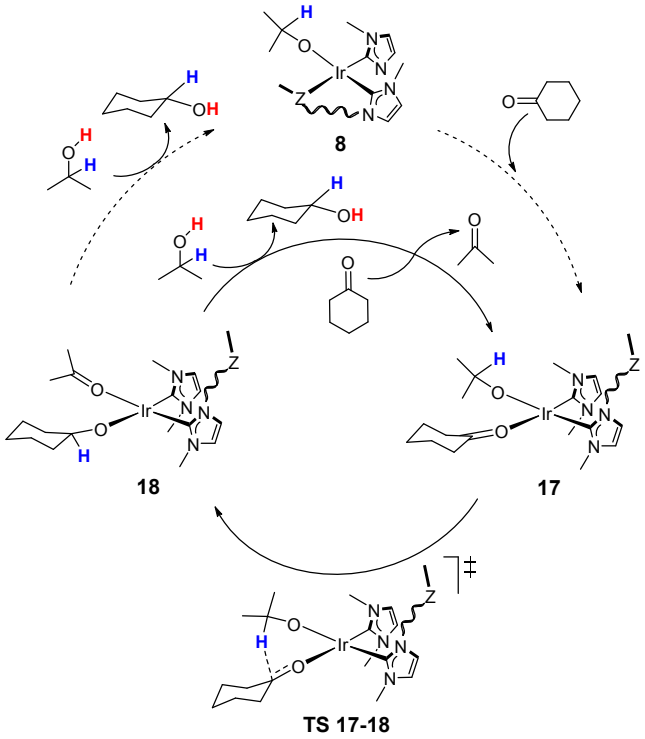


**Figure 11.** Catalytic cycle for a MPV-like concerted mechanism. The dotted arrows involve the N-substituent on the carbene ligand and should make a difference in the catalytic activity of different ligands. The solid arrows represent the proposed cycle, independent on the nature of the substituent on the carbene ligand.

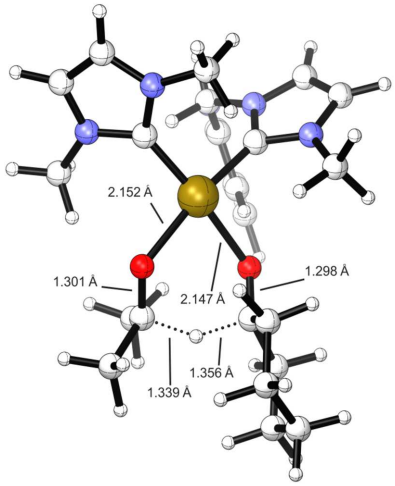


**Figure 12.** Transition state structure **TS17a-18a** for a MPV-like concerted mechanism. Some relevant distances are shown.

In light of the above described results, both mechanism pathways seem to be possible. The last step, which closes the cycles, could occur through intermediate **8** for both ligands and either in a MPV-like mechanism (Figure 11) or through hydrido square planar intermediates formed via β-elimination mechanism (Figure 8). Involvement of intermediate **8** would lead to very different catalytic activities for the two different N-substituents (pyridin-2-ylmethyl and 2-methoxybenzyl) given the larger coordination ability of pyridine compared to the ether group and the larger stability of the chelate ring compared to the one formed with the ether donor, which in both cases should open to form the next species in the catalytic cycle. In consequence, if the species **8** were part of either a MPV-like mechanism (Figure 11) or an hydride square planar intermediates via β-elimination mechanism (Figures 8), the catalytic activity should be significantly lower for complex $\mathbf{5}^+$ than for $\mathbf{4}^+$, as very different energy span would be involved for either catalyst (see all the comparative of energies for the different routes in Figure S10 included in the Supporting Information). On the contrary, our experimental observations show that the catalysts [Ir(cod)(MeIm∩Z)$_2$][X] (∩Z = 2-methoxybenzyl, $\mathbf{4}^+$; pyridine-2-ylmethyl, $\mathbf{5}^+$, quinolin-8-ylmethy, $\mathbf{6}^+$) have all a similar activity which is roughly independent on the N-substituent on the carbene ligand (Table 3). Attending to these experimental results the species **8** should be outside of both cycles, and the catalytic reactions should close by 2-propanol alcoholysis (hydride mechanism, Figure 8) or by 2-propanol alcoholysis plus substrate addition (MPV-like mechanism, Figure 11). This suggests that the substitution processes that close the cycle avoiding intermediate 8 must be faster than the reorganization process for reforming the chelating ring in the presence of a large excess of substrate. In other case, the greater coordinating ability of the pyridine substituent should lead to a larger energy span in any of both mechanisms

compared to the benzylether substituent, which is in disagreement with the experimental results.

The energy span[41] for both mechanisms is rather small. For the catalyst containing the ligand MeIm(pyridin-2-ylmethyl) an energy span of 18.1 kJ/mol for the hydride mechanism and 31.7 kJ/mol for the MPV-like mechanism are found. For the catalyst containing the ligand MeIm(2-methoxybenzyl) they amount to 12.8 and 52.3 kJ/mol respectively. In the first case (∩Z = pyridin-2-ylmethyl) it is clear that the difference is small enough to consider that both mechanisms could operate simultaneously. The case where ∩Z = 2-methoxybenzyl deserves some additional comments. The difference of *ca.* 21 kJ/mol in activation energy in the MPV cycle for both catalysts (31.7 vs 52.3 kJ/mol), although small, is somewhat unexpected. The transition state corresponds to the direct transfer of hydrogen form isopropoxide to cyclohexanone and the electronic environment must be similar for both ligands, and the difference must have a steric or conformational origin. Lledós, Maseras et al.[42] have pointed out that the error introduced by conformational diversity can range values of less than 4 kJ/mol to around 42 kJ/mol. The simplification introduced in one the ligands and the possible conformational freedom of the uncoordinated sidearms of the carbene ligands suggest that both mechanisms are in a similar range of energy spans and both could be operating simultaneously. On the other hand the large excess of cyclohexanone can shift the balance to the formation of **17** in the MPV cycle in preference to agostically coordinated **12** in the hydride pathway.

In order to shed some light on the operating mechanism we have studied the in situ generation of the active species under catalytic hydrogen transfer conditions by ESI and MALDI- TOF mass spectrometry.[13,43] The ESI mass spectrum of a $1x10^{-3}$ M solution of

complex [Ir(cod){MeIm(pyridin-2-ylmethyl)}$_2$]$PF_6$ (**5**·**PF$_6$**) in 2-propanol under argon atmosphere showed the molecular ion at m/z 647.1 (80%), and the peaks at m/z 539.1 (34 %) and 471.1 (7%) that correspond to the fragments $[Ir(MeIm\cap Z)_2]^+$ and $[Ir(cod)(MeIm\cap Z)]^+$ (∩Z = pyridin-2-ylmethyl), respectively. The ESI mass spectrum after addition of a solution of KOH (1:5) and heating at 80 ºC for 15 min showed the peak corresponding to $[Ir(MeIm\cap Z)_2]^+$ although neither the hydrido $[IrH(MeIm\cap Z)_2]$ nor the alocoxo $[Ir(OR)(MeIm\cap Z)_2]$ intermediates were observed. Both species were not observed either in the MALDI-TOF mass spectra, even in linear mode.[44] In addition, the $^1$H NMR of a $d^8$-THF solution of **5**·**PF$_6$** containing K$^i$PrO (1:5) after heating at 80 ºC for 30 min did not show any hydrido resonance. Taking into account the outstanding stability of the hydrido model intermediate **14**, $[IrH(ImMe_2)(MeIm\cap Z)]$ (Figure 8), that might be recognized as the resting state in the hydride mechanism, the failure in the identification of the related species $[IrH(MeIm\cap Z)_2]$ under catalytic conditions, and the small calculated energy span difference between both mechanism (*ca.* 13 kJ/mol) suggest that the transfer hydrogenation by catalyst **5**$^+$, based on pyridin-2-ylmethyl functionalized NHC ligands, could proceed through a MPV-like mechanism.

## Conclusions

Unbridged biscarbene $[Ir(cod)(MeIm\cap Z)_2]^+$ complexes having functionalized N-heterocyclic ligands with 2-methoxybenzyl, pyridin-2-ylmethyl and quinolin-8-ylmethyl wingtips have been prepared. Restricted rotation about the C(carbene)-Ir bond in these complexes results in two interconverting diasteromers derived from the relative disposition of the functionalized NHC ligands, up-down and up-up, having antiparallel and parallel arrangement of the carbene ligands, respectively. The equilibrium between

both rotational isomers has been fully characterized by means of 2D-EXSY NMR spectroscopy. In the solid state both complexes exhibit an antiparallel disposition of the carbene ligands that minimize the steric repulsions between the bulkiest substituents. The complexes are efficient catalyst precursor for the transfer hydrogenation of cyclohexanone in 2-propanol/KOH exhibiting comparable activity independently both of the wingtip type at the NHC ligands and the counterion. Mechanistic studies on the formation of the active catalytic species evidenced that the hydrogenation of the 1,5-cyclooctadiene ligand to cyclooctene is a prerequisite for the generation of key bis-carbene iridium(I)-alkoxo intermediates. DFT calculations on two possible operating mechanisms: the formation of a hydride intermediate via a β-elimination step and a direct hydrogen transfer with the metal center acting as Lewis acid (MPV-like concerted mechanism), have shown that both mechanism pathways seem to be possible. In the catalytic system based on 2-methoxybenzyl functionalized NHC ligands the hydride mechanism seems to be favored. However, the model simplification and the possible conformational effects of the uncoordinated wingtip of the NHC ligands suggest a similar range of energy spans and then, both mechanisms might be operative. In sharp contrast, the small calculated energy span difference between both mechanisms for the catalyst based on NHC ligands having a pyridin-2-ylmethyl wingtip, along with the no direct observation of a hydrido resting state predicted to be highly stable, suggest that hydrogen transfer catalysis could proceed through a MPV-like mechanism.

## Experimental Section

**Scientific Equipment.** C, H and N analyses were carried out in a Perkin-Elmer 2400 Series II CHNS/O analyzer. Infrared spectra were recorded on a FT-Perkin-Elmer

Spectrum One spectrophotometer using Nujol mulls between polyethylene sheets. $^{1}H$ and $^{13}C\{^{1}H\}$ NMR spectra were recorded on a Bruker Avance 300 (300.1276 MHz and 75.4792 MHz) or Bruker Avance 400 (400.1625 MHz and 100.6127 MHz) spectrometers. NMR chemical shifts are reported in ppm relative to tetramethylsilane and referenced to partially deuterated solvent resonances. Coupling constants (*J*) are given in Hertz. Spectral assignments were achieved by combination of $^{1}H$-$^{1}H$ COSY, $^{13}C$ APT and $^{1}H$-$^{13}C$ HSQC experiments. MALDI-TOF mass spectra were obtained on a Bruker MICROFLEX spectrometer using DIT, ditranol, 1,8-dihidroxi-9,10-dihydroanthracen-9-one, as matrix.[45] Electrospray mass spectra (ESI-MS) were recorded on a Bruker MicroTof-Q using sodium formiate as reference. Conductivities were measured in *ca.* 5 $10^{-4}$ M acetone solutions of the complexes using a Philips PW 9501/01 conductimeter.

The catalytic reactions were analyzed on an Angilent 4890 D system equipped with an HP-INNOWax capillary column (0.4 μm film thickness, 25 m x 0.2 mm i. d.) using mesitylene as internal standard. Organic compounds were identified by Gas Chromatography-Mass Spectrometry (GC/MS) using an Agilent 6890 GC system with an Agilent 5973 MS detector, equipped with a polar capillary column HP-5MS (0.25 μm film thickness, 30 m x 0.25 mm i. d.).

**Synthesis.** All experiments were carried out under an atmosphere of argon using Schlenk techniques. Solvents were distilled immediately prior to use from the appropriate drying agents or obtained from a Solvent Purification System (Innovative Technologies). Oxygen-free solvents were employed throughout. $CDCl_3$, and $CD_2Cl_2$ were dried using activated molecular sieves, methanol-$d_4$ (<0.02% $D_2O$) was purchased from Euriso-top and used as received. MeImH (*N*-methyl-imidazole) was obtained from

Sigma-Aldrich and distilled prior to use. The substrates were obtained from common commercial sources and used as received, or re-crystallized or distilled prior to use depending on their purity. The imidazolium salts [MeImH(2-methoxybenzyl)]Br (**1**),[13] [MeImH(pyridin-2-ylmethyl)]Br (**2**),[18] and [MeImH(quinolin-8-ylmethyl)]$PF_6$ (**3**);[19] and the iridium starting materials $[Ir(\mu\text{-}Cl)(cod)]_2$[46] and $[\{Ir(\mu\text{-}OMe)(cod)\}_2]$,[47] were prepared according to literature procedures.

**General method for the synthesis of complexes [Ir(cod)(MeIm∩Z)$_2$]Br (∩Z = 2-methoxybenzyl, 4·Br; pyridin-2-ylmethyl, 5·Br)**. The compounds were prepared following the method described by Herrmann.[22a] To a suspension of $[Ir(\mu\text{-}Cl)(cod)]_2$ (0.15 mmol) in ethanol (15 mL) a solution of NaH (1.0 mmol) in ethanol (5 mL) was slowly added and stirred at room temperature for 30 min. Then, the corresponding imidazolium salt [(MeImH∩Z]Br (0.6 mmol) was added and the suspension stirred for 72 h. The solvent was pumped off and the residue extracted with $CH_2Cl_2$ (3 x 5 mL). The solution was concentrated under vacuum to 1mL and then, n-hexane (4 mL) was added to give the compounds as orange-yellow solids that were washed with n-hexane (3 x 2 mL) and dried under vacuum.

**[Ir(cod){MeIm(2-methoxybenzyl)}$_2$]Br (4·Br)**. $[Ir(\mu\text{-}Cl)(cod)]_2$ (100 mg, 0.149 mmol), [MeImH(2-methoxybenzyl)]Br (**1**) (169 mg, 0.596 mmol) and NaH (24.1 mg, 1.01 mmol). Yield: 81%. Anal. Calcd for $C_{32}H_{40}BrN_4O_2Ir$: C, 48.97; H, 5.14; N, 7.14. Found: C, 49.08; H, 5.20; N, 7.12. **Isomer 4a$^+$**: $^1$H NMR (298 K, acetone-$d_6$): $\delta$ 7.35 (m, 2H, CH Ar), 7.14 (d, $J$ = 2.0, 2H, CH Im), 7.11 (d, $J$ = 7.6, 2H, CH Ar), 7.04 (d, $J$ = 2.0, 2H, CH Im), 6.85 (m, 2H, CH Ar), 6.62 (dd, $J$ = 7.5, 1.5, 2H, CH Ar), 5.54 (AB system, $\delta_A$ = 5.63, $\delta_B$ = 5.43, $J_{AB}$ = 15.0, 4H, $NCH_2$), 4.29 (td, $J$ = 7.8, 2.4, 2H, CH cod), 4.15 (s, 6H, MeIm), 3.91 (s, 6H, OMe), 3.66 (m, 2H, CH cod), 2.42–2.16 (m, 4H, $CH_2$

cod), 1.95–1.72 (m, 4H, $CH_2$ cod). $^{13}C\{^1H\}$ NMR (298K, acetone-$d_6$): $\delta$ 178.28 (NCN), 157.86 (C Ar), 130.35, 128.46 (CH Ar), 125.22 (C Ar), 124.32, 122.43 (CH Im), 121.44, 111.58 (CH Ar), 78.92, 74.74 (CH cod), 55.99 (OMe), 50.21 ($NCH_2$), 38.17 (MeIm), 34.06, 29.82 ($CH_2$ cod). **Isomer 4b$^+$**: $^1H$ NMR (298 K, acetone-$d_6$): $\delta$ 7.35 (m, 2H, CH Ar), 7.33 (d, $J$ = 2.0, 2H, CH Im), 7.11 (d, $J$ = 7.6, 2H, CH Ar), 6.99 (d, $J$ = 2.0, 2H, CH Im), 6.85 (m, 2H, CH Ar), 6.52 (dd, $J$ = 7.5, 1.5, 2H, CH Ar), 5.39 (AB system, $\delta_A$ = 5.82, $\delta_B$ = 4.92, $J_{AB}$ = 15.0, 4H, $NCH_2$), 3.93 (s, 6H, MeIm), 3.98 (m, 2H, CH cod), 3.90 (s, 6H, OMe), 3.89 (m, 2H, CH cod), 2.42–2.16 (m, 4H, $CH_2$ cod), 1.95–1.72 (m, 4H, $CH_2$ cod). $^{13}C\{^1H\}$ NMR (298K, acetone-$d_6$): $\delta$ 178.41 (NCN), 157.72 (C Ar), 130.16, 127.96 (CH Ar), 125.61 (C Ar), 124.27, 122.80 (CH Im), 121.49, 111.52 (CH Ar), 76.80, 76.48 (CH cod), 55.95 (OMe), 49.94 ($NCH_2$), 38.83 (MeIm), 31.96, 31.84 ($CH_2$ cod). MS (MALDI-Tof, $CH_2Cl_2$): *m/z* = 705.3 $[M]^+$. $\Lambda_M$ (acetone): 79 $\Omega^{-1}$ cm$^2$ mol$^{-1}$.

**[Ir(cod){MeIm{pyridin-2-ylmethyl)}$_2$]Br (5·Br)**. [MeImH(pyridin-2-ylmethyl)]Br (**2**) (100 mg, 0.394 mmol), [Ir(μ-Cl)(cod)]$_2$ (66.1 mg, 0.098 mmol) and NaH (26.5 mg, 0.663 mmol). Yield: 87%. Anal. Calcd for $C_{28}H_{34}BrN_6Ir$: C, 46.28; H, 4.72; N, 11.56. Found: C, 46.37; H, 4.81; N, 11.52. **5a$^+$**: $^1H$ NMR (298 K, $CD_2Cl_2$): $\delta$ 8.47 (d, $J$ = 4.5, 2H), 7.63 (td, $J$ = 7.7, 1.7, 2H), 7.25 (m, 2H), 7.06 (d, $J$ = 7.8, 2H) (CH py), 6.95 (d, $J$ = 1.9, 2H, CH Im), 6.86 (d, $J$ = 1.9, 2H, CH Im), 5.63 (AB system, $\delta_A$ = 5.73, $\delta_B$ = 5.53, $J_{AB}$ = 17.5, 4H, $NCH_2$), 4.20 (td, $J$ = 2.2, 7.6, 2H, CH cod), 3.69 (s, 6H, MeIm), 3.57 (m, 2H, CH cod), 2.31–2.12 (m, 4H, $CH_2$ cod), 1.80 (m, 4H, $CH_2$ cod). $^{13}C\{^1H\}$ NMR ($CD_2Cl_2$): $\delta$ 178.03 (NCN), 155.33 (C py), 149.59, 137.16, 123.40, 123.09 (CH py), 122.96, 121.35 (CH Im), 78.97, 74.88 (CH cod), 55.32 ($NCH_2$), 37.47 (MeIm), 33.16, 29.40 ($CH_2$ cod). **5b$^+$**: $^1H$ NMR (298 K, $CD_2Cl_2$): $\delta$ 8.52 (d, $J$ = 4.5, 2H), 7.69 (td, $J$ =

7.7, 1.7, 2H), 7.25 (m, 2H) (CH py), 7.18 (d, *J* = 1.9, 2H, CH Im), 6.99 (d, *J* = 7.8, 2H, CH py), 6.95 (d, *J* = 1.9, 2H, CH Im), 6.87 (d, *J* = 1.9, 2H, CH Im), 5.48 (AB system, $\delta_A$ = 5.82, $\delta_B$ = 15.0, $J_{AB}$ = 5.2, 4H, $NCH_2$), 4.02 (s, 6H, MeIm), 3.95 (m, 2H, CH cod), 3.83 (m, 2H, CH cod), 2.31–2.12 (m, 4H, $CH_2$ cod), 2.03 (m, 4H, $CH_2$ cod). $^{13}C\{^1H\}$ NMR ($CD_2Cl_2$): $\delta$ 177.88 (NCN), 155.30 (C py), 149.86, 137.19 (CH py), 123.45, 121.80 (CH Im), 121.80, 121.56 (CH py), 76.69, 76.85 (CH cod), 55.17 ($NCH_2$), 38.30 (MeIm), 31.33, 31.14 ($CH_2$ cod). MS (MALDI-Tof, $CH_2Cl_2$): *m/z* = 647.3 $[M]^+$, 539.2 $[M - C_8H_{12}]^+$. $\Lambda_M$ (acetone): 92 $\Omega^{-1}$ cm$^2$ mol$^{-1}$.

**Synthesis of [Ir(cod)(MeIm∩Z)$_2$]PF$_6$ (∩Z = 2-methoxybenzyl, 4·PF$_6$; pyridin-2-ylmethyl, 5·PF$_6$)**. $KPF_6$ was added to solutions of [Ir(cod){MeIm(2-methoxybenzyl)}$_2$]Br (**4·Br**) or [Ir(cod){MeIm{pyridin-2-ylmethyl)}$_2$]Br (**5·Br**) in $CH_2Cl_2$ (10 mL) and the mixture stirred for 2 h at room temperature. The inorganic salts were removed by filtration and the resulting orange solutions were concentrated under vacuum to 1 mL. The addition of $Et_2O$ (3 mL) gave the compounds as orange solids that were washed with $Et_2O$ (3 x 2 mL) and dried in vacuo.

**[Ir(cod){MeIm(2-methoxybenzyl)}$_2$]PF$_6$ (4·PF$_6$)**. $KPF_6$ (23.5 mg, 0.128 mmol) and **4·Br** (100 mg, 0.128 mmol). Yield: 92%. Anal. Calcd for $C_{32}H_{40}F_6N_4O_2PIr$: C, 45.22; H, 4.74; N, 6.59. Found: C, 45.34; H, 4.83 N, 6.57. IR (thin film, cm$^{-1}$): ν($PF_6$) = 840 (s). $^{31}P\{^1H\}$ NMR (acetone-$d_6$): $\delta$ -144.26 ppm.

**[Ir(cod){MeIm{pyridin-2-ylmethyl)}$_2$]PF$_6$ (5·PF$_6$)**. $KPF_6$ (25.3 mg, 0.138 mmol) and **5·Br** (100 mg, 0.138 mmol). Yield: 91%. Anal. Calcd for $C_{28}H_{34}F_6N_6PIr$: C, 42.47; H, 4.33; N, 11.61. Found: C, 43.25; H, 4.42; N, 11.64. IR (thin film, cm$^{-1}$): ν($PF_6$) = 840 (s). $^{31}P\{^1H\}$ NMR ($CD_2Cl_2$): $\delta$ -144.31 ppm.

**Preparation of [Ir(cod){MeIm{MeIm(quinolin-8-ylmethyl)}$_2$]PF$_6$ (6·PF$_6$).** Portions of KO$^t$Bu (28.3 mg, 0.252 mmol) were added to a stirred suspension of [MeImH(quinolin-8-ylmethyl)]PF$_6$ (**3**) (100 mg, 0.252 mmol) in tetrahydrofurane at room temperature. After stirring of the mixture for 30 min, [Ir(μ-Cl)(cod)]$_2$ (42.3 mg, 0.063 mmol) was added in one portion. The reaction mixture was stirred overnight. Removal of the solvent and crystallization from acetone/Et$_2$O at -10 ºC afforded an orange microcrystalline solid that was washed with Et$_2$O (3 x 2 mL) and dried under vacuum. Yield: 80%. Calculated analysis for $C_{36}H_{38}F_6IrN_6P$: C, 48.48; H, 4.29; N, 9.42. Found: C, 48.59; H, 4.35; N, 9.44. **6a**$^+$: $^1$H NMR (298 K, $CDCl_3$): $\delta$ 8.91 (dd, $J$ = 4.2, 1.8, 2H), 8.24 (dd, $J$ = 8.3, 1.8, 2H), 7.83 (d, $J$ = 8.2, 2H), 7.52 (dd, $J$ = 8.3, 4.2, 2H), 7.43 (dd, $J$ = 8.3, 4.2, 2H), 7.36 (m, 2H), 7.03 (m, 2H) (CH quinol), 6.82 (d, $J$ = 1.8, 2H, CH Im), 6.80 (d, $J$ = 1.8, 2H, CH Im), 6.09 (AB system, $\delta_A$ = 6.23, $\delta_B$ = 5.95, $J_{AB}$ = 15.0, 4H, NCH$_2$), 4.42 (t, $J$ = 7.7, 2H, CH cod), 3.64 (s, 6H, MeIm), 3.55 (m, 2H, CH cod), 2.1 (m, 4H, CH$_2$ cod), 1.8 (m, 4H, CH$_2$ cod). $^{13}$C{$^1$H} NMR ($CDCl_3$): $\delta$ 177.76 (NCN), 150.22 (CH quinol), 145.64 (C quinol), 136.77 (CH quinol), 133.77 (C quinol), 128.43 (CH quinol), 128.18 (C quinol), 127.54, 126.48 (CH quinol), 123.36, 121.88 (CH Im), 121.54 (CH quinol), 78.90, 74.24 (CH cod), 50.90 (NCH$_2$), 37.60 (MeIm), 33.58, 29.36 (CH$_2$ cod). **6b**$^+$: $^1$H NMR (298 K, $CDCl_3$): $\delta$ 8.79 (dd, $J$ = 4.1, 1.8, 2H), 8.13 (dd, $J$ = 8.3, 1.8, 2H), 7.75 (d, $J$ = 8.2, 2H), 7.45 (dd, $J$ = 8.3, 4.2, 2H), 7.36 (m, 2H) (CH quinol), 7.11 (d, $J$ = 1.8, 2H, CH Im), 6.73 (m, 2H, CH quinol), 6.67 (d, $J$ = 1.8, 2H, CH Im), 5.84 (AB system, $\delta_A$ = 6.36, $\delta_B$ = 5.32, $J_{AB}$ = 16.5, 4H, NCH$_2$), 4.11 (s, 6H, MeIm), 4.03 (m, 2H, CH cod), 3.94 (m, 2H, CH cod), 2.34–2.15 (m, 4H, CH$_2$ cod), 1.92 (m, 4H, CH$_2$ cod). $^{13}$C{$^1$H} NMR ($CDCl_3$): $\delta$ 177.93 (NCN), 149.88 (CH quinol), 145.57 (C quinol), 136.38 (CH quinol), 134.46, 128.18 (C quinol), 127.98,

126.70, 126.34 (CH quinol), 123.50, 121.68 (CH Im), 121.54 (CH quinol), 76.54, 76.39 (CH cod), 50.53 ($NCH_2$), 38.35 (MeIm), 31.54, 31.18 ($CH_2$ cod). $^{31}P\{^1H\}$ NMR ($CD_2Cl_2$): $\delta$ -144.31 ppm. MS (MALDI-Tof, $CH_2Cl_2$): *m/z* = 747.4 $[M]^+$, 637.6 $[M - C_8H_{12}]^+$, 524.2 $[M - C_{14}H_{13}N_3]^+$. $\Lambda_M$ (acetone): 91 $\Omega^{-1}cm^2mol^{-1}$.

**Preparation of [IrH$_2${$\kappa^2$*C,N*-MeIm(pyridin-2-ylmethyl)}$_2$]PF$_6$ (7·PF$_6$)**. A solution of [Ir(cod){MeIm(pyridin-2-ylmethyl)}$_2$]$PF_6$ (**5·PF$_6$**) (100 mg, 0.140 mmol) in acetonitrile (20 mL) was stirred in a Parr reactor at 10 bar of hydrogen pressure and 60 ºC for 48 h. At the end of this time, the pale yellow solution recovered from the reactor was concentrated to 1 mL. Addition of diethyl ether (3 mL) resulted in the formation of a yellow solid that was washed with cold diethyl ether (2 x 2 mL) and dried under vacuum. Yield: 81%. Anal. Calcd for $C_{20}H_{24}F_6N_6PIr$: C, 35.04; H, 3.53; N, 12.26. Found: C, 35.11; H, 3.61; N, 12.29. $^1H$ NMR (298 K, $CD_3CN$): $\delta$ 8.94 (d, *J* = 4.2, 1H, CH py), 7.92 (m, 3H, CH py), 7.34 (m, 2H, CH Im and CH py), 7.27 (m, 2H, CH Im and CH py), 7.14 (m, 1H, CH py), 7.04 (d, *J* = 2.0, 1H, CH Im), 6.98 (t, *J* = 7.5, 1H, CH py), 6.91 (d, *J* = 2.0, 1H, CH Im), 5.58 – 5.09 (m, 4H, $NCH_2$), 3.27 (s, 3H, MeIm), 2.22 (s, 3H, MeIm), –9.66 (d, *J* = 5.6, 1H, Ir–H), –20.12 (d, *J* = 5.6, 1H, Ir–H). $^{13}C\{^1H\}$ NMR (298K, $CD_3CN$): $\delta$ 174.15, 173.85 (NCN), 155.78, 157.85 (C py), 161.10, 155.09, 138.93, 138.56, 138.24, 126.18, 125.86 (CH py), 125.54 (CH Im), 122.56 (CH py), 121.76, 121.65, 120.81 (CH Im), 58.74, 58.43 ($NCH_2$), 37.63, 34.78 (MeIm). $^{31}P\{^1H\}$ NMR ($CD_3CN$): $\delta$ -144.26 ppm. MS (MALDI-Tof, matriz DCTB, $CH_2Cl_2$): *m/z* = 541.2 $[M]^+$. $\Lambda_M$ (acetone): 91 $\Omega^{-1}$ $cm^2$ $mol^{-1}$.

**General Procedure for Transfer Hydrogenation Catalysis.** The catalytic transfer hydrogenation reactions were carried out under an argon atmosphere in thick glass reaction tubes fitted with a greaseless high-vacuum stopcock. In a typical experiment,

the reactor was charged with a solution of the substrate (5 mmol) in 2-propanol (4.5 mL), internal standard (mesitylene, 70 μL, 0.5 mmol), base (104 μL, 0.025 mmol of a KOH solution 0.24 M in 2-propanol) and the catalyst (0.005 mmol, 0.1 mol%). The resulting mixture was stirred at room temperature until complete solution of the catalyst and then placed in a thermostatized oil bath at the required temperature, typically 80 ºC. Conversions were determined by Gas Chromatography analysis under the following conditions: column temperature 35 ºC (2 min) to 220 ºC at 10 ºC/min with a flow rate of 1 mL/min using ultra pure He as carrier gas.

**Determination of the kinetic parameters by 2D-EXSY NMR spectroscopy**. The kinetic parameters for the equilibrium $\mathbf{5a}^+ \leftrightarrows \mathbf{5b}^+$ in $\mathbf{5}\cdot\mathbf{Br}$ were obtained from the $^1$H 2D-EXSY NMR spectra (500.13 MHz) with a mixing time of 500ms optimized for 300 K by using a gradient-selected NOESY program from Bruker (noesygpph). The integrations for the exchange cross-peaks between the methyl resonances of the functionalized NHC ligands in both diasteromers were processed using the EXSYCalc program to compute the rate constants $k_1$ and $k_{-1}$ ($s^{-1}$).[48] The rotational barriers, $\Delta G_1^{\#}$ and $\Delta G_{-1}^{\#}$ ($kJ\cdot mol^{-1}$), were calculated from the chemical exchange-rate constants obtained from ESXYCalc, $k_1$ and $k_{-1}$, using the Eyring equation, $k = (k_B T/h)\exp(-\Delta G^{\#}/RT)$. The activation parameters, $\Delta H^{\#}$ and $\Delta S^{\#}$, were calculated from a linear least-squares fit of ln(k/T) vs 1/T. The uncertainties in $\Delta H^{\#}$ and $\Delta S^{\#}$ were computed from the error propagation formulas derived from the Eyring equation by Girolami and co-workers.[49] The total uncertainty in the determination of $k$ was assumed to be 5%. The estimated uncertainty in the temperature measurements was 1K.

**Calculation details.** DFT calculations have been carried out with Gaussian 09[50] using the B3PW91 functional with a 6-31G** basis set for all atoms but Ir where the

LANL2DZ basis set and pseudopotential has been used supplemented with an additional f function[51]. All the minima have been characterized by frequency calculations. The structures in Figures 9 and 12 have been depicted using CYLview. 1.0b.[52]

**Crystal Structure Determination of Complexes [Ir(cod){MeIm(2-metoxybenzyl)}$_2$]PF$_6$ (4·PF$_6$), [Ir(cod){MeIm(pyridin-2-ylmethyl)}$_2$]Br** (**5·Br**), **and [Ir(cod){MeIm(quinolin-8-ylmethyl)}$_2$]PF$_6$ (6·PF$_6$)**. X-ray diffraction data were collected at 100(2) K with graphite-monochromated Mo K$\alpha$ radiation ($\lambda$ = 0.71073 Å) using narrow ω rotation (0.3º) on a Bruker APEX DUO (**4·PF$_6$** and **5·Br**) or a Bruker SMART APEX CCD (**6·PF$_6$**) diffractometers. Intensities were integrated and corrected for absorption *effects* with SAINT-PLUS and SADABS programs[53] included in APEX2 package. The structures were solved by direct methods with SHELXS-97.[54] Refinement by full-matrix least-squares on $F^2$, was performed with SHELXL-97.[55] Hydrogen atoms were included in calculated positions and refined with displacement and positional riding parameters. In **4·PF$_6$** and **5·Br** complexes, an analysis of the disordered solvent region has been performed with SQUEEZE program.[56] Particular details concerning specific refinement are listed below.

*Crystal data for **4·PF$_6$***: $C_{32}H_{40}F_6IrN_4O_2P$, $M$ = 849.88; orange plate, 0.116 × 0.037 × 0.030 mm$^3$, triclinic, $P\bar{1}$, $a$ = 10.946(4), $b$ =11.935(4), $c$ =14.097(5) Å, $\alpha$ = 101.745(7), β = 107.631(6), $\gamma$ = 101.754(7)º; $Z$ =2; $V$ = 1647.4(10) Å$^3$; $D_c$ = 1.713 g/cm$^3$; $\mu$ = 4.171 mm$^{-1}$; minimum and maximum absorption correction factors: 0.525 and 0.828; $2\theta_{max}$ = 42.72º; 9840 collected reflections, 3674 unique ($R_{int}$ = 0.0747); number of data/restraints/parameters 3674/0/419; final GOF 1.010; $R1$ = 0.0540 (3133 reflections, $I > 2\sigma(I)$); $wR2$ = 0.1435 for all data; largest difference peak 2.841 e/Å$^3$. When

convergence is achieved residual density peaks higher than 1 e/Å$^3$ are found close to the iridium atom. They have no chemical sense. Sample crystallizes in tiny plates, mutually stuck. Several crystals were tested before selecting the one used for the data collection. Most of them have shown to be slightly twinned. Eventually, a very weakly diffracting crystal was selected. No detectable intensity was observed over 43º and therefore this value has been used as cut-off during the integration process.

*Crystal data for* ***5·Br***: $2(C_{28}H_{34}BrIrN_6)\cdot O_2H\cdot CH_2Cl_2$, $M$ = 1556.39; orange plate, 0.099 × 0.082 × 0.043 mm$^3$, triclinic, $P\bar{1}$, $a$ = 10.390(6), $b$ =14.148(8), $c$ =20.021(11) Å, $\alpha$ = 88.505(8), β = 89.648(8), $\gamma$ = 78.507(8)º; $Z$ =2; $V$ = 2883(3) Å$^3$; $D_c$ = 1.793 g/cm$^3$; $\mu$ = 6.141 mm$^{-1}$; minimum and maximum absorption correction factors: 0.432 and 0.717; $2\theta_{max}$ = 58.98º; 30565 collected reflections, 14370 unique ($R_{int}$ = 0.0562); number of data/restraints/parameters 14370/0/662; final GOF 0.879; $R1$ = 0.0498 (9250 reflections, $I > 2\sigma(I)$); $wR2$ = 0.1215 for all data; largest difference peak 2.168 e/Å$^3$. When convergence is achieved residual density peaks higher than 1 e/Å$^3$ are found close to the iridium atom. They have no chemical sense.

*Crystal data for* ***6·PF$_6$***: $C_{36}H_{38}F_6IrN6P\cdot 0.5(C_4H_{10}O)$, $M$ = 928.95; orange prism, 0.265 × 0.235 × 0.211 mm$^3$, monoclinic, $P2_1/c$, $a$ = 12.1243(9), $b$ = 19.5765(15), $c$ = 15.7923(12) Å, β = 102.8500(10)º; $Z$ =4; $V$ = 3654.4(5) Å$^3$; $D_c$ = 1.688 g/cm$^3$; $\mu$ = 3.767 mm$^{-1}$; minimum and maximum absorption correction factors: 0.407 and 0.528; $2\theta_{max}$ = 56.82º; 42545 collected reflections, 8498 unique ($R_{int}$ = 0.0239); number of data/restraints/parameters 8498/14/469; final GOF 1.052; $R1$ = 0.0233 (7514 reflections, $I > 2\sigma(I)$); $wR2$ = 0.0569 for all data; largest difference peak 1.426 e/Å$^3$.

**Acknowledgements.** Financial support from the Spanish Ministry of Economy and Competitiveness (MINECO/FEDER, Project: CTQ2013-42532-P) and Diputación

General de Aragón (DGA/FSE-E07) is gratefully acknowledged. JFT thanks the Spanish MICINN for a predoctoral fellowship. The authors thankfully acknowledge the resources from the supercomputer "Caesaraugusta" (node of the Spanish Supercomputer Network), technical expertise and assistance provided by BIFI - Universidad de Zaragoza.

**Supporting Information Available.** Selected NMR spectra, experimental procedure for the determination of the kinetic parameters by 2D-EXSY spectroscopy, computational information: calculated data (B3LYP) for catalytic intermediates (DFT_structures.xyz), and X-ray crystallographic information files containing full details of the structural analysis of complexes **4**·**PF$_6$**, **5**·**Br** and **6**·**PF$_6$** (CIF format). This material is available free of charge via the Internet at http://pubs.acs.org.

## References

(1) (a) Kwong, F. Y.; Chan, A. S. C. *Synlett* **2008**, 1440–1448. (b) Braunstein P.; Naud, F. *Angew. Chem. Int. Ed.* **2001**, *40*, 680–699. (d) Bader, A.; Lindner, E. *Coord. Chem. Rev.* **1991**, *108*, 27–110.

(2) (a) Riener, K.; Bitzer, M. J.; Pöthig, A.; Raba, A.; Cokoja, M.; Herrmann, W. A.; Kühn, F. E. 10 *Inorg. Chem.* **2014**, 1021/ic5016324. (b) Schaper, L. -A.; Hock, S. J.; Herrmann, W. A.; Kühn, F. E. *Angew. Chem. Int. Ed.* **2013**, *52*, 270–289. (c) Kühl, O. *Functionalised N-heterocyclic Carbene Complexes*; Wiley: Chichester, U. K., 2010. (d) Normand, A. T.; Cavell, K. J. *Eur. J. Inorg. Chem.* **2008**, 2781–2800. (e) Mühlhofer, M.; Strassner, T.; Herrmann, W. A. *Angew. Chem. Int. Ed. Engl.* **2002**, *41*, 1745–1747.

(3) (a) Petronilho, A.; Llobet, A.; Albrecht, M. *Inorg. Chem.* **2014**, 10.1021/ic501894u. (b) Nolan, S. P. *Acc. Chem. Res.* **2011**, *44*, 91–100. (c) Jiménez, M. V.; Pérez-Torrente, J. J.; Bartolomé, M. I.; Gierz, V.; Lahoz, F. J.; Oro, L. A. *Organometallics* **2008**, *27*, 224–234. (d) Lee, H. M.; Lee, C.-C.; Cheng, P.-Y. *Curr. Org. Chem.* **2007**, *11*, 1491–1524.

(4) (a) Gülcemal, S.; Daran, J.-C.; Çetinkaya, B. *Inorg. Chim. Acta* **2011**, *365*, 264–268. (b) Yang, X.; Fei, Z.; Geldbach, T. J.; Phillips, A. D.; Hartinger, C. G.; Li, Y.; Dyson, P. J. *Organometallics* **2008**, *27*, 3971–3977. (c) Ohta, H.; Fujihara, T.; Tsuji, Y. *Dalton Trans.* **2008**, 379–385. (d) Kuhlman, E.; Himmler, S.; Giebelhaus, H.; Wasserscheid, P. *Green Chem.* **2007**, *9*, 233–242.

(5) (a) Iglesias, M.; Pérez-Nicolas, M.; Sanz Miguel, P. J.; Polo, V.; Fernández-Álvarez, F. J.; Pérez-Torrente, J. J.; Oro, L. A. *Chem. Commun.* **2012**, *48*, 9480–9482. (b) Jiménez, M. V.; Pérez-Torrente, J. J.; Bartolomé, M. I.; Vispe, E.; Lahoz, F. J.; Oro, L. A. *Macromolecules* **2009**, *42*, 8146–8156. (c) César, V.; Bellemin-Laponnaz, S.; Gade, L. H. *Chem. Soc. Rev.* **2004**, *33*, 619–636. (d) Albrecht, M.; van Koten, G. *Angew. Chem., Int. Ed.* **2001**, *40*, 3750–3781. (e) Beletskaya, I. P.; Cheprakov, A. V. *Chem. Rev.* **2000**, *100*, 3009–3066.

(6) (a) Campos, J.; Hintermair, U.; Brewster, T. P.; Takase, M. K.; Crabtree, R. H. *ACS Catal.* **2014**, *4*, 973–985. (b) Sluijter, S. N.; Elsevier, C. J. *Organometallics* **2014**, *33*, 6389–6397. (c) Bala, M. D.; Ikhile, M. I. *J. Mol. Catal. A: Chemical* **2014**, *385*, 98–105. (d) Humphries, M. E.; Pecak, W. H.; Hohenboken, S. A.; Alvarado, S. R.; Swenson, D. C.; Domski, G. J. *Inorg. Chem. Commun.* **2013**, *37*, 138–

143. (e) Horn, S.; Albrecht, M. *Chem. Commun.* **2011**, *47*, 8802–8804. (f) Wylie W. N. O.; Lough, A. J.; Morris, R. H. *Organometallics* **2009**, *28*, 6755–6761. (g) Gladiali, S.; Alberico, E. *Chem. Soc. Rev.* **2006**, *35*, 226–236.

(7) (a) Hintermair, U.; Campos, J.; Brewster, T. P.; Pratt, L. M.; Schley, N. D.; Crabtree, R. H. *ACS Catal.* **2014**, *4*, 99–108. (b) Gülcemal, D.; Gökçe, A. G.; Gülcemal, S.; Çetinkaya, B. RSC Adv. **2014**, *4*, 26222-26230. (c) Blanco, M.; Álvarez, P.; Blanco, C.; Jiménez, M. V.; Fernández-Tornos, J.; Pérez-Torrente, J. J.; Oro, L. A.; Menéndez, R. *ACS Catal.* **2013**, *3*, 1307–1317. (d) Dunsford, J. J.; Tromp, D. S.; Cavell, K. J.; Elsevier, C. J.; Kariuki, B. M. *Dalton Trans.* **2013**, *42*, 7318–7329. (e) Azua, A.; Mata, J. A.; Peris, E.; Lamaty, F.; Martínez, J.; Colacino, E. *Organometallics* **2012**, *31*, 3911–3919. (f) Saidi, O.; Williams, J. M. J. *Top. Organomet. Chem.* **2011**, *34*, 77–106. (g) Sanz, S.; Benitez, M.; Peris, E. *Organometallics* **2010**, *29*, 275–277. (h) Albrecht, M. *Chem. Commun.* **2008**, *31*, 3601–3610. (i) Pontes da Costa, A.; Viciano, M.; Sanaú, M.; Merino, S.; Tejeda, J.; Peris, E.; Royo, B. *Organometallics* **2008**, *27*, 1305–1309. (j) Kownacki, I.; Kubicki, M.; Szubert, K.; Marciniec, B. *J. Organomet. Chem.* **2008**, *693*, 321–328. (k) Hahn, F. E.; Holtgrewe, C.; Pape, T.; Martin, M.; Sola, E.; Oro, L. A. *Organometallics* **2005**, *24*, 2203–2209. (l) Albrecht, M.; Crabtree, R. H.; Mata, J. A.; Peris, E. *Chem. Commun.* **2002**, 32–33. (m) Hillier, A. C.; Lee, H. M.; Stevens, E. D.; Nolan, S. P. *Organometallics* **2001**, *20*, 4246–4252.

(8) (a) Danopoulos A. A. in *N-Heterocyclic-Carbenes in Transition Metal Catalysis and Organocatalysis, Catalysis by Metal Complexes* 32, Cazin, C. S. J. Ed.; Springer: Berlin, 2011, 2, 23–61. (b) Yang, L.; Kruger, A.; Neels, A.; Albrecht, M. *Organometallics* **2008**, *27*, 3161–3171. (c) Peris, E.; Mas-Marzá, E.; Sanaú, M. *Inorg.*

*Chem.* **2005**, *44*, 9961–9967. (d) Miecznikowski, J. R.; Crabtree, R. H. *Organometallics* **2004**, *23*, 629–631. (e) Miecznikowski, J. R.; Crabtree, R. H. *Polyhedron* **2004**, *23*, 2857–2872. (f) Albrecht, M.; Miecznikowski, J. R.; Samuel, A.; Faller, J. W.; Crabtree, R. H. *Organometallics* **2002**, *21*, 3596–3604.

(9) Türkmen, H.; Pape, T.; Hahn, F. E.; Çetinkaya, B. *Eur. J. Inorg. Chem.* **2008**, 5418–5423.

(10) Binobaid, A.; Iglesias, M.; Beetstra, D.; Dervisi, A.; Fallis, I.; Cavell, K. J. *Eur. J. Inorg. Chem.* **2010**, 5426–5431.

(11) Samec, J. S. M.; Bäckvall, J. -E.; Andersson, P. G.; Brandt, P. *Chem. Soc. Rev.* **2006**, *35*, 237–248.

(12) (a) Kubas, G. J. *J. Organomet. Chem.* **2014**, *751*, 33–49. (b) Wang, C. -Y.; Fu, C. -F.; Liu , Y. -H.; Peng , S. -M.; Liu, S. -T. *Inorg. Chem.*, **2007**, *46*, 5779–5786. (c) Dahlenburg , L.; Götz R. Inorg. *Chem. Commun.* **2003**, *6*, 443–446.

(13) Jiménez, M. V.; Fernández-Tornos, J.; Pérez-Torrente, J. J.; Modrego, F. J.; Winterle, S.; Cunchillos, C.; Lahoz, F.; Oro, L. A. *Organometallics* **2011**, *30*, 5493–5508.

(14) (a) B. Jokić, N. B.; Zhang-Presse, M.; Goh, L. M. S.; Straubingera, C. S.; Bechlarsb, B. Herrmann, W. A.; Kühn, F. E. *J. Organomet. Chem.* **2011**, *696*, 3900–3905. (b) Diez, C.; Nagel, U. *Appl. Organometal. Chem.* **2010**, *24*, 509–516.

(15) Handgraaf, J. -W.; Reek, J. N. H.; Meijer, E. J. *Organometallics* **2003**, *22*, 3150–3157.

(16) Danthi, S. N.; Hill, R. A. *J. Heterocyclic Chem.* **1997**, *34*, 835–844.

(17) Ray, L.; Shaikh, M. M.; Ghosh, P. *Organometallics* **2007**, *26*, 958–964.

(18) McGuinness, D. S.; Cavell, K. J. *Organometallics* **2000**, *19*, 741–748.

(19) (a) Sun, J. -F.; Chen, F.; Dougan, B. A.; Xu, H. -J.; Cheng, Y.; Li, Y. -Z.; Chen, X. -T.; Xue, Z. -L. *J. Organomet. Chem.* **2009**, *694*, 2096–2105. (b) Peng, H. M.; Webster, R. D.; Li, X. *Organometallics* **2008**, *27*, 4484–4493.

(20) Hintermair, U.; Englert, U.; Leitner, W. *Organometallics* **2011**, *30*, 3726–3731.

(21) Voutchkova, A. M.; Feliz, M.; Clot, E.; Eisenstein, O.; Crabtree, R. H. *J. Am. Chem. Soc.* **2007**, *129*, 12834–12846.

(22) (a) Frey, G. D.; Rentzsch, C. F.; von Preysing, D.; Scherg, T.; Mühlhofer, M.; Herdtweck, E.; Herrmann, W. A. *J. Organomet. Chem.* **2006**, *691*, 5725–5738. (b) Rentzsch, C. F.; Tosh, E.; Herrmann, W. A.; Kühn, F. E. *Green Chem.*, **2009**, *11*, 1610–1617.

(23) Alcarazo, M.; Roseblade, S. J.; Cowley, A. R.; Fernández, R.; Brown, J. M.; Lassaletta, J. M. *J. Am. Chem. Soc.* **2005**, *127*, 3290–3291.

(24) Messerle, B. A.; Page, M. J.; Turner, P. *Dalton Trans.* **2006**, 3927–3933.

(25) Leung, C. H.; Incarvito, C. D.; Crabtree, R. H. *Organometallics* **2006**, *25*, 6099–6107.

(26) (a) Pérez-Torrente, J. J.; Angoy, M.; Gómez-Bautista, D.; Palacios, A.; Jiménez, M. V.; Modrego, F. J.; Castarlenas, R.; Lahoz, F.; Oro, L. A. *Dalton Trans*. **2014**, *43*,

14778–14786. (b) Jiménez, M. V.; Lahoz, F. J.; Lukešová, L.; Miranda, J. R.; Modrego, F. J.; Nguyen, D. H.; Oro, L. A.; Pérez-Torrente J. J. *Chem. Eur. J.* **2011**, *17*, 8115–8128. (c) Nikitin, K.; Müller-Bunz, H.; Ortin, Y.; Muldoon, J.; McGlinchey, M. J. *J. Am. Chem. Soc.* **2010**, *132*, 17617–17622. (d) Amaya, T.; Sakane, H.; Muneishi, T.; Hirao, T. *Chem. Commun.* **2008**, 765–767. (c) Carmichael, D.; Ricard, L.; Seeboth, N.; Brown, J. M.; Claridge, T. D. W.; Odell, B. *Dalton Trans.* **2005**, 2173–2181. (d) Cossío, F. P.; De la Cruz, P.; De la Hoz, A.; Langa, F.; Martín, N.; Prieto, P.; Sánchez, L. *Eur. J. Org. Chem.* **2000**, 2407–2415.

(27) Chianese, A. R.; Li, X.; Janzen, M. C.; Faller, J. W.; Crabtree R. H. *Organometallics* **2003**, *22*, 1663–1667, and references therein.

(28) Busetto, L.; Cassani, M. C.; Femoni, C.; Mancinelli, M.; Mazzanti, A.; Mazzoni, R.; Solinas G. *Organometallics* **2011**, *30*, 5258–5272.

(29) Enders, D.; Gielen, H. *J. Organomet. Chem.* **2001**, *617*, 70–80.

(30) See for example: (a) Ros, A.; Alcarazo, M.; Iglesias-Sigüenza, J.; Díez, E.; Álvarez, E.; Fernández, R.; Lassaletta, J. M. *Organometallics* **2008,** *27*, 4555–4564, and references therein. (b) Herrmann, W. A.; Gooβen, L. J.; Spiegler, M. *J. Organomet. Chem.* **1997**, *547*, 357–366.

(31) Allen, F. H. *Acta Crystallogr.* **2002**, *B58*, 380–388.

(32) See for example: Tang, C. Y.; Thompson, A. L.; Aldridge, S. *J. Am. Chem. Soc.* **2010**, *132*, 10578, and references therein.

(33) Burling S.; Mahon, M. F.; Reade, S. P.; Whittlesey, M. K. *Organometallics* **2006**, *25*, 3761–3767.

(34) Herrmann, W. A.; Frey, G. D.; Herdtweck, E.; Steinbeck, M. *Adv. Synt. Catal.* **2007**, *349*, 1677–1691).

(35) Iglesias, M.; Sanz-Miguel, P. J.; Polo, V.; Fernández-Álvarez, F. J.; Pérez-Torrente, J. J.; Oro, L. A. *Chem. Eur. J.* **2013**, *19*, 17559–17566.

(36) Stylianides, N.; Danopoulos, A. A.; Tsoureas, N. *J. Organomet. Chem.* **2005**, *690*, 5948–5958.

(37) Mata, J. A.; Chianese, A. R.; Miecznikowski, J. R.; Poyatos, M.; Peris, E.; Faller, J. W.; Crabtree, R. H. *Organometallics* **2004**, *23*, 1253–1263.

(38) Gründemann, S.; Kovacevic, A.; Albrecht, M.; Faller, J. W.; Crabtree, R. H. *Chem. Commun.* **2001**, 2274–2275.

(39) Comas-Vives, A.; Ujaque, G.; Lledós, A. *Organometallics* **2007**, *26*, 4135–4144.

(40) Zhao, J.; Hesslink, H.; Hartwig, J.F. *J. Am. Chem. Soc.* **2001**, *123*, 7220–7227.

(41) (a) Kozuch, S.; Shaik, S. J *J. Phys. Chem. A* **2008**, *112*, 6032–6041 (b) Kozuch, S.; Martin, J.M.L. *ChemPhysChem.* **2011**, *12*, 1413–1418

(42) Besora, M.; Braga, A. A. C.; Ujaque, G.; Maseras, F.; Lledós, A. *Theor. Chem. Acc.* **2011**, *128*, 639–646

(43) (a) Vicent, C.; Viciano, M.; Mas-Marzá, E.; Sanau, M.; Peris, E. *Organometallics* **2006**, *25*, 3713–3720. (b) Bakhtiar, R; Hop, C. *J. Phys. Org. Chem.* **1999**, *12*, 511–527.

(44) The MALDI-TOF analysis performed in linear mode conduct to less fragmentation, and meta-stable species might be observed.

(45) Ulmer, L.; Mattay, J.; Torres-García, H. G.; Luftmann, H. Eur. J. Mass Spectrom. 2000, 6, 49–52.

(46) Herde, J. L.; Lambert, J. C.; Senoff, C. V. *Inorg. Synth.* **1974**, *15*, 18–20.

(47) Usón, R.; Oro, L. A.; Cabeza, J. A. *Inorg. Synth.* **1985**, *23*, 126–127.

(48) Cross-peaks were integrated and processed with the EXSYCalc software distributed by Mestrelab research (http://www.mestrec.com).

(49) Morse, P. M.; Spencer, M. D.; Wilson, S. R.; Girolami, G. S. *Organometallics* **1994**, *13*, 1646–1655.

(50) *Gaussian 09, Revision A.1*, Frisch, M. J.; Trucks, G. W.; Schlegel, H. B.; Scuseria, G. E.; Robb, M. A.; Cheeseman, J. R.; Scalmani, G.; Barone, V.; Mennucci, B.; Petersson, G. A.; Nakatsuji, H.; Caricato, M.; Li, X.; Hratchian, H. P.; Izmaylov, A. F.; Bloino, J.; Zheng, G.; Sonnenberg, J. L.; Hada, M.; Ehara, M.; Toyota, K.; Fukuda, R.; Hasegawa, J.; Ishida, M.; Nakajima, T.; Honda, Y.; Kitao, O.; Nakai, H.; Vreven, T.; Montgomery, Jr., J. A.; Peralta, J. E.; Ogliaro, F.; Bearpark, M.; Heyd, J. J.; Brothers, E.; Kudin, K. N.; Staroverov, V. N.; Kobayashi, R.; Normand, J.; Raghavachari, K.; Rendell, A.; Burant, J. C.; Iyengar, S. S.; Tomasi, J.; Cossi, M.;

Rega, N.; Millam, N. J.; Klene, M.; Knox, J. E.; Cross, J. B.; Bakken, V.; Adamo, C.; Jaramillo, J.; Gomperts, R.; Stratmann, R. E.; Yazyev, O.; Austin, A. J.; Cammi, R.; Pomelli, C.; Ochterski, J. W.; Martin, R. L.; Morokuma, K.; Zakrzewski, V. G.; Voth, G. A.; Salvador, P.; Dannenberg, J. J.; Dapprich, S.; Daniels, A. D.; Farkas, Ö.; Foresman, J. B.; Ortiz, J. V.; Cioslowski, J.; Fox, D. J. *Gaussian, Inc.*, Wallingford CT, 2009.

(51) Ehlers, A.; Böhme, M.; Dapprich, S.; Gobbi, A.; Höllwarth, A.; Jonas, V.; Köhler, K.; Stegmann, R.; Veldkamp, A.; Frenking, G. *Chem. Phys. Letters* **1993**, *208*, 111–114.

(52) Legault, C. Y. CYLview, 1.0b, (http://www.*cylview*.org), Université de Sherbrooke, **2009**.

(53) SAINT+ Software for CCD Diffractometers; Bruker AXS: Madison, WI, 2000. Sheldrick, G. M. *SADABS Program for Correction of Area Detector Data*; University of Göttingen: Göttingen, Germany, 1999.

(54) G. M. Sheldrick, *Acta Crystallogr., A*, **1990**, *46*, 467–473.

(55) G. M. Sheldrick, *Acta Crystallogr., A*, **2008**, *64*, 112–122.

(56) Sluis, P. v.d.; Spek, A. L. *Acta Crystallogr., A* **1990**, *46*, 194–201.

**For the Table of Contents**